Institute of Radiofrequency and Microwave Engineering

Master Thesis

Statistical Channel Modeling Approach for Professional Wireless Microphone Systems

Gonzalo Ruiz Lantero
Matrikelnummer: 2694180

Tutor: Dipl.-Ing. Sven Dortmund
Coordinator: José María Molina García-Pardo

Hannover, June 2010

Contents

1 Introduction **1**

2 Statistical Channel Modelling **3**

2.1 Channel Fading and Multipath propagation 5

2.1.1 Signal time spreading 6

2.1.2 Time variance of the channel 9

2.1.3 Indoor radio channel 10

2.2 Saleh-Valenzuela model 11

2.2.1 Model development setup 11

2.2.2 SVM description 12

2.3 The SCM and SCME channel models 15

2.4 WINNER channel model 16

2.4.1 WINNER Channel model description 16

2.4.2 Network layout and system level 19

2.4.3 Propagation scenarios 21

2.5 COST 259/273 channel models 22

2.5.1 COST 259 22

2.5.2 COST 273 23

2.6 The IEEE 802.11 TGn channel model 23

3 WINNER implementation **24**

3.1 Winner Matlab code 25

3.1.1 Antenna model for WINNER channel simulations 27

3.1.2 Network layout parameters 30

3.1.3 General simulation parameters 33

3.1.4 Channel impulse response generation 36
3.2 Code adaptation for Professional Wireless Microphone System, PWMS . 42
3.2.1 Code adaptation for PWMS antennas 43
3.2.2 Code adaptation for PWMS network layout parameters 46
3.2.3 Code adaptation for PWMS general simulation parameters 51

4 PWMS scenario 55
4.1 Hanover Congress Center, HCC 55
4.1.1 Real HCC hall 56
4.1.2 WINNER virtual HCC hall 60
4.2 Data analysis 67
4.3 WINNER channel model simulations 75
4.3.1 IEM WINNER analysis 76
4.3.2 MS velocity analysis 81

5 Summary, conclusions and outlook 86

Bibliography 89

1 Introduction

Since its inception, some 60 years ago, the wireless audio transmission systems have revolutionized the possibilities in the world of the entertainment industry and have encouraged the deployment of artistic performances free of impediments, for transmission of audio signals wirelessly by removing the connecting cables so annoying and prone to failures. Belonging to these systems, the professional wireless microphone systems, PWMS, have been imposed at the expense of other systems, especially in scenarios for concerts, plays, conferences, sport events or to provide news coverage.

The major drawback of these systems is that they are very sensitive to radio interference, whether by random degrading effects or by other applications located near or in the same frequency band. For this reason it is very important to study these PWMS applications in order to ensure their proper operation free of interference, especially in big events where there is a high probability of interference from other applications. These studies are focusing on evaluating the feasibility of using alternative frequency bands for these applications. Currently, the PWMS operates within the UHF band from 470MHz to 862MHz, sharing this portion of spectrum with broadcasting applications. Due to the continuing digitalization of these broadcasting applications, it is very likely to be carry out a restructuring of the frequency bands in which they operate, including the PWMS applications. To ensure interference-free employment of PWMS applications, employability of the PWMS applications over alternatives frequency bands was evaluated, focusing in particular, at 1500MHz L-band and other less common use frequencies such as 1800MHz

An earlier research, [Vos08], addressed this issue. To carry out this task, two different PWMS application areas were examined. These experiments were based on taking measures in a real scenario, for both types of the applications areas. To validate these measures, a previously selected channel model, the Saleh-Valenzuela channel model, was used. One

of these PWMS applications was focused on the use of the so-called bodypack which are attached to the body. This device could act as a transmitter and a receiver. In particular, acting as a receiver, allows, to the person who carries it, listen to himself or others through the so-called in ear monitoring, IEM. The thesis presented in this document extends the research described above, by simulating by computer the PWMS application in which the bodypack acts as a receiver. The channel model used for this purpose is the WINNER channel model. This channel model differs in many aspects from the Saleh-Valenzuela model, so it will be necessary a comparison between them to verify the equivalence of both experiments.

This thesis is structured in three parts. In the first, the theoretical concepts concerning to the wireless transmission and the degrading effects that affect them, are explained, as well as, the description of the Saleh-Valenzuela channel model, in section 2.2, and the WINNER channel model, in section 2.4. The second part corresponds with chapter 3. It explains all the parameters and options provided by the WINNER channel model and how to use them in order to simulate different wireless applications, including the PWMS application under study. The last part is developed along chapter 4 and 5. In section 4.1, the PWMS application scenarios are described. The interpretation of [Vos08] results is performed in section 4.2, while the WINNER channel model simulations and comparisons are described in subsequent sections of Chapter 4. To finish, final conclusions are presented in Chapter 5.

2 Statistical Channel Modelling

As stated in the introduction section, the main goal of this thesis is to describe a PWMS application using the Saleh-Valenzuela channel model and the WINNER channel model and comparing them. In order to get this done, knowledge of the useful wireless communications concepts (in terms of PWMS applications) is essential. This chapter introduces these basic concepts required: the channel parameters description, the nature of the degrading effects that happen inside the channel, and the influence of them on the transmitted signal along the path between the transmitter and receiver antennas. In subsequent sections, the Saleh-Valenzuela channel model and the WINNER channel model are described in detail, as well as, other standardized channel models.

In a wireless communication channel, an electromagnetic wave travels from the receiver to the transmitter by air. This channel behaves like a linear filter, that is, the transmitter signal suffers modifications when it passes through the filter, obtaining a receiver signal as a linear function of the transmitter signal. If $h(t)$ is the channel that acts as a filter and $x(t)$ and $y(t)$ are the transmitter and receiver signals respectively, according to [Skl01], $y(t)$ can be expressed as the convolution between $x(t)$ and $h(t)$.

$$y(t) = x(t) * h(t). \tag{2.1}$$

$h(t)$ is also called the channel impulse response, CIR. Fig2.1 shows a basic scheme of a wireless communication system, where the impulse response is represented as the propagation medium between the transmitter, Tx, and the receiver, Rx, and, also, as a linear filter. Both representations are equivalent.

In practice, the scheme shown in Fig.2.1 is often more complex. The number of transmitter and receivers may vary depending on the application. Thus, there are wireless applications

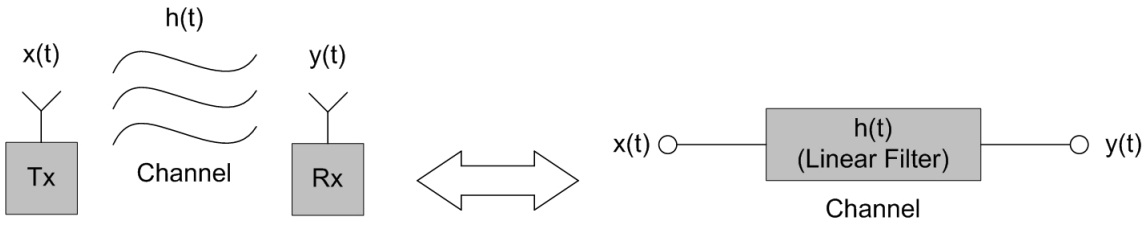

Figure 2.1: Basic scheme of a wireless communication system

with multiple inputs and outputs (MIMO channels), with only one transmitter and receiver, i.e, single input single output (SISO channels), a combination of both, either multiple input single output (MISO channels) or applications with one single input and multiple outputs (SIMO channels). Specifically, the PWMS application under consideration in this thesis, works on a SISO channel.

The optimal conditions for any communication system are that the received signal, $y(t)$, is the same as the transmitted signal, $x(t)$, but this, unfortunately never happens. Studying the communication channel, can draw conclusions about how it affects the transmitted signal. The knowledge of the degradation effects of a channel allows to act in a manner that can mitigate, as much as possible, the impact of the channel on the received signal. In wireless systems the main degradation effects caused by the channel are due to the propagation environment, that is, the physical structure that surrounds the transmitter (or transmitters) and receiver (or receivers). Channel modelling aims to study different environments over which wireless communications take place. These studies conclude in a description of each environment. These descriptions are called channel models and predict how a signal can be affected by a specific environment. Mainly, there are two types of channel models:

- Statistical channel models.These channel models are based on signal propagation measurement campaigns in various real environments. The data obtained is analyzed using statistical methods. This analysis gets the occurrence probability of each random parameter involved in the signal propagation of the environment under consideration. Statistical channel models do not bear in mind the geometry of a physical environment. As conclusion, the statistical channel models are based on statistical descriptions of a physical behavior. Examples of statistical channel mod-

els that are described further, are: Saleh-Valenzuela model, 3GPP SCM model and WINNER model.

- Deterministic channel models. According to [Alm], deterministic channel models aim to reproduce the physical radio propagation process for a given environment. The deterministic models store in files, called environment databases, the geometric and electromagnetic characteristics of the environment and the radio communication links. The corresponding propagation process can be simulated through computer programs. Due to the high accuracy of these models, deterministic models may be used to replace statistical models when there is not enough time to set up a measurement campaign or when it is very difficult to measure in the real world. The most important deterministic models for radio propagation are the ray tracing models, which are based in geometrical optics theory.

The following subsections delve into the degradation or fading effects that occur in a wireless communication channel, and describe some examples of statistical channel models.

2.1 Channel Fading and Multipath propagation

The main propagation effect that occurs on a signal, along its travel from the transmitter to the receiver, is the degradation or fading. As specified in [Skla][Has], there are two types of fading: large-scale fading and small-scale fading. Large-scale fading represents the average signal power attenuation or path loss due to motion over large areas. This phenomenon is affected by prominent land contours like mountains, forests, groups of buildings, etc, located between transmitter and receiver. Small-scale fading refers to the dramatic changes in the signal amplitude and phase due to small changes (half wavelength) which occur between the transmitter and the receiver. The PWMS application that is analyzed in this thesis is located inside a big conference hall where the effects of large-scale fading are not relevant. Therefore, this chapter focuses only on small-scale fading which manifests itself in two mechanisms: signal time spreading and time-variant behavior of the channel.

2.1.1 Signal time spreading

Signal time spreading is the result of the multipath propagation or multipath fading, which is explained in this paragraph. The signal, in its travel along the channel, is affected by mainly 3 basic degrading effects. They are reflection, diffraction, and scattering. The first one occurs when a propagating wave impinges on a smooth surface with very large dimensions compared to the signal wavelength, λ, whose mathematical expression is

$$\lambda = \frac{v}{f} = \frac{c}{f}, \tag{2.2}$$

where v is the velocity of the propagated wave. In PWMS applications it is assumed that the transmission is by air, so v can be approximated at the light velocity, c. f is the frequency of the transmitted signal.

Going back to the degrading effects, diffraction happens when the traveler signal is obstructed by a dense body with large dimensions compared to λ, causing secondary waves which are formed behind the obstructing body. Finally, scattering occurs when a radio wave impinges on either a large rough surface or either any surface whose dimensions are much smaller than λ, causing dispersion, in all directions, of the reflected energy. The environment elements that produce reflection, diffraction or scattering are called scatters. For example, in a PWMS application case working on 1GHz as an example, that is, λ is around $30cm$, tables or people walking inside the room can produce reflection and diffraction respectively, and also, a single microphone or an inhomogeneous wall surface, may be the cause of the scatter effect. Because of these 3 mechanisms, the transmitted signal most often reaches the receiver by more than one way or path, resulting in a phenomenon known as multipath propagation or multipath fading. These paths consist of several main rays due to reflection and diffraction. Sometimes, when the transmitter and receiver have an unobstructed path between them, there is a direct main ray that is the first to reach the receiver. This main ray is called line of sight (LOS) ray. The remaining main rays will appear progressively depending on the path length. These main rays do not travel directly from the transmitter to the receiver and therefore are called obstructed line of sight (OLOS) ray or non line of sight (NLOS) ray. Each main ray breaks up in other rays due to the scattering produced by the environment structure. The resulting rays from each main

ray arrive with very close delays, producing a series of delayed and attenuated rays. The continuous time domain representation of the channel impulse response is the envelope of the chronological sum of all the rays, as can be seen in fig2.2. This figure represents, also, the channel power delay profile, PDP, which means the intensity of the signal received as a function of time delay.

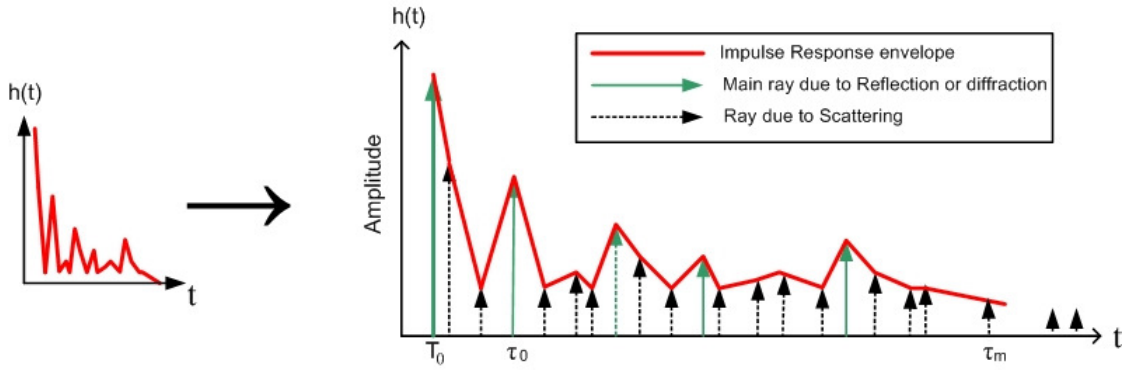

Figure 2.2: Example of a channel impulse response

Accoding to [Sak] the channel impulse response, CIR, can be calculated via

$$h(t) = \sum_{n=1}^{m} A_n \delta(t - \tau_n) e^{-j\varphi_n} \tag{2.3}$$

δ is the Dirac delta whose representation can be seen in fig.2.3. Eq.2.3 is the sum of m δ's, when each δ (referenced by an index n) is characterized by amplitude A, phase φ, and arrival time or delay τ. In other words, eq.2.3 is the mathematical expression of the channel impulse response seen in fig.2.2. From fig.2.2, and assuming that the transmitter and receiver have an unobstructed path between them, T_0 represents the instant when the most direct ray (LOS ray) reach the receiver. The time interval from T_0 to τ_m is called Delay Spread, T_m. τ_0 is the first moment of the delay spread, that is, is the moment when the second main ray, due to the first significant reflection or diffraction, reaches the receiver. The period of time between τ_0 and τ_m is called RMS Delay Spread, τ_{RMS}, and gives an overview of the propagation environment. Large values of τ_{RMS} mean strong echoes with long delays due to, e.g., far scatters in a wide rural environments. In the same way, small values of τ_{RMS} mean, also, small values of τ_m, that is, insignificant long delay echoes

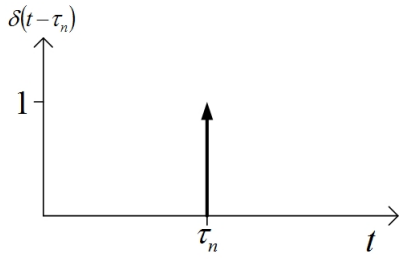

Figure 2.3: Dirac Delta at instant τ_n

typical of small environments like rooms. As reported in [Sak], τ_{RMS} can be expressed as

$$\tau_{RMS} = \sqrt{[\sum_{n=1}^{m}(\tau_n - \tau_0 - T_0)^2 A_n^2] / \sum_{n=1}^{m} A_n^2}. \tag{2.4}$$

τ_{RMS} determines the coherent bandwidth, B_C. B_C is a statistical measure in the frequency domain over which the channel can be considered flat, that is, that passes all spectral components with approximately equal gain and linear phase. In other words, represents a frequency range over which frequency components are affected by the channel in a way that they exhibit, or not, fading. According to [Sak],

$$B_C \approx 1/50\tau_{RMS}. \tag{2.5}$$

In this case, and according to [Cav00], the discrete time representation of the CIR, eq.2.3, is just a tapped delay line, TDL, with spacing τ. From that equation, each Delta is called "tap", and each "tap" is defined via its relative delay, amplitude and phase.

Signal time spreading derives in two fading effects: Frequency-selective fading and flat fading. Frequency-selective fading occurs when all the spectral components of the signal are not affected equally by the channel. In other words, occurs whenever the coherent bandwidth is less than the signal bandwidth, W, $B_C < W$. For example, if this condition occurs, the received multipath components of a symbol extend beyond the symbol's time duration, thus causing channel-induced intersymbol interference (ISI). Flat fading occurs when all the signal's spectral components are affected by the channel in a similar manner, $B_C > W$. Flat fading produces a substantial reduction in signal-to-noise ratio, SNR.

2.1.2 Time variance of the channel

The channel time-variant behavior is caused by the movement of the scenario elements such as rotating antennas or, e.g. people walking between transmitter and receiver. It means that the channel impulse response changes in time, making the channel non-stationary. Fig.2.4 shows graphically this effect, as well as the time evolution of the first rays of the channel impulse response. M_i is the ith instant of time, t', where the measure of channel impulse response take place. As it is shown in the next subsection, this mechanism can

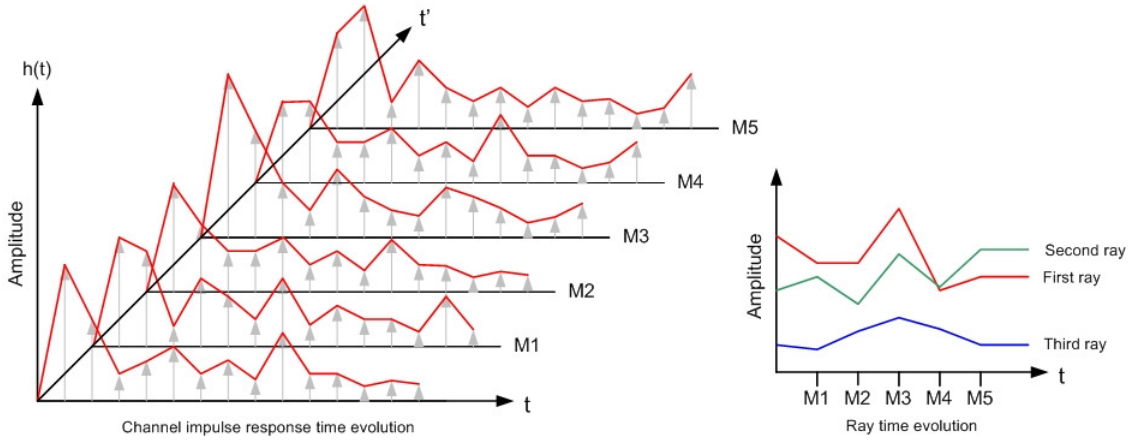

Figure 2.4: Time evolution of the channel impulse response.

be neglected in most outdoor environments, where the main scatters (buildings, hills, etc) are fixed. Time variance of the channel derives in two fading effects: fast fading and slow fading. Fast fading occurs when the time duration for which the channel impulse response is more or less invariant (it behaves in a correlated manner) is short compared to the time duration of a transmitted signal, causing distortion in the baseband pulse. Slow fading, by contrast, occurs when the time duration for which the channel behaves in a correlated manner is long compared to the time duration of the signal transmitted.

In brief, small-scale fading produces two effects, time variance of the channel and signal time spreading. Each effect derives in two types of fading, fast fading and slow fading, for the first and frequency-selective fading and flat fading for the last one. According to [Sklb], frequency-selective fading and fast fading are more damaging than flat fading and slow fading because, for the same SNR, the first two present higher values in the bit error

probability, P_B, than the others. Moreover, all these fading effects affect the signal differently, depending on the environment of the wireless application under consideration. The next subsection characterizes, in terms of fading effects, the typical PWMS environments.

2.1.3 Indoor radio channel

Concert halls, recording studios or conference halls (the case of this thesis), are examples of typical PWMS environments. They have one thing in common, they are indoor channels. The differences between indoor environments and outdoor environments are mainly due to the scatters and the size of the application area. Indoor channels differ from the outdoor channels in the following aspects:

- Channel time evolution. In indoor channels, the scatters that produce the multipath propagation might be not fixed. The movement of one of them produces temporal variations of the CIR for the same channel. Therefore, indoor channels are also called non-stationary channels. On the contrary, the multipath propagation of some outdoor channels is due to fixed scatters like mountains, buildings or fences. This is the typical environment of rural or urban areas where the traffic effect is not relevant. These kinds of channels are stationary channels. In conclusion, indoor channels have a time variant behavior.

- Doppler shift effect. Consists of the shift in frequency and wavelength of waves, which are the result of a source moving with respect to the medium, a receiver moving with respect to the medium, or even a moving medium. In outdoor channels, the transmitter or receiver may be located inside moving elements with high velocities like cars or trains, making the Doppler shift effect very relevant. In indoor channels, the velocity of moving elements is always very small, so the Doppler shift is negligible in this case.

- Delay spread. Since the area of indoor channels is usually smaller than the outdoor channels area, the different paths in which the signal travels from the transmitter to the receiver are smaller in indoor channels. This results in a shorter delay spread. As

reported in [Has], the outdoor channels delay spread are between several microseconds and several hundreds of microseconds, while an indoor channel delay spread is around several hundreds of nanoseconds.

- Correlation. In indoor environments, the multipath components of the same CIR calculated, are so close between them, causing them to be not independent. Spatial correlations govern the amplitudes, the time arrivals and the phases.

2.2 Saleh-Valenzuela model

The Saleh-Valenzuela model, SVM, first presented in [Sal] is a statistical MIMO channel model approach. Saleh and Valenzuela proposed a statistical explanation for clustered characteristics of measured received power delay profiles in indoor environment. Their statistical model is an extension of the Turin channel model [Tur]. SVM presents the channel behavior of a medium-size office building and is featured by:

- Enough flexibility to permit reasonably accurate fitting of the measured channel responses.
- Simple to use in simulation and analysis of various indoor communications setups.
- Extendable (by adjusting its parameters) to represent the channel within others buildings.

The following subsections describe, first, the layout and conditions in which this model has been developed and its mathematical formulation. Later, the statistical characteristics and the description of the channel model output format is explained.

2.2.1 Model development setup

The Saleh-Valenzuela model has been developed inside a medium-size office building with external walls made of steel beams and glass. The rooms contain typical metal office furniture and/or laboratory equipment. For this experiment, the transmitter antennas are placed in the corridors of the building, while the receiver antennas are located inside

rooms. The frequency of the transmitter signal using for measurements is 1.5GHz and the vertically polarized antennas present an omnidirectional radiation pattern in the horizontal plane.

The transmitted signal is represented by $x(t)$

$$x(t) = p(t)e^{j(wt+\phi)}, \tag{2.6}$$

where $p(t)$ is the baseband pulse shape,ω is $2\pi f$ where f is the frequency and ϕ is an arbitrary phase. The channel, $h(t)$,

$$h(t) = \sum_k \beta_k e^{j\theta_k} \delta(t - \tau_k), \tag{2.7}$$

is formed by multiple subpaths or rays which are characterized in terms of amplitude β_k, propagation delay τ_k, and associated phase shift θ_k, where k is the subpath or ray index (from 0 to ∞). Eq.2.7 represents the time discrete impulse response channel. The received signal is the time convolution of $x(t)$ and $h(t)$. The following subsection describes the model based on the measurements results.

2.2.2 SVM description

According to eq.2.7, the goal of SVM is predict the β_k and τ_k pairs, under the assumption that the phase angles θ_k are statistically independent random variables with and uniform distribution over [0, 2π), and the subpath amplitude, β_k, are mutually independent. This multipath model is based in the fact that the subpaths or rays arrive in clusters. The cluster arrival time T_l is the arrival time of the first ray of lth cluster, and is modeled as a Poisson arrival process with some fixed rate Λ. Within each cluster, subsequent rays also arrive according to a Poisson process with another fixed rate λ. The ray arrival times are represented by τ_{kl}, when k is the number of the ray that is inside lth cluster. T_l and τ_{kl} are described by the independent interarrival exponential probability density functions presented in the next equations:

$$p(T_l|T_{l-1}) = \Lambda exp[-\Lambda(T_l - T_{l-1})], l > 0, \tag{2.8}$$

$$p(\tau_{kl}|\tau_{(k-1)l}) = \lambda exp[-\lambda(\tau_{kl} - \tau_{(k-1)l})], k > 0. \tag{2.9}$$

In the same way, β_{kl} is the amplitude of the kth ray of the lth cluster, and its probability distribution follows the Rayleigh probability density function described by the equation 2.10.

$$p(\beta_{kl}) = (2\beta kl/\overline{\beta_{kl}^2})exp(-\beta_{kl}^2/\overline{\beta_{kl}^2}). \tag{2.10}$$

Fig.2.5 is a representation, along the time, of the channel impulse response which is parametricied by the concepts explained above. Although mean the same thing, the eq.2.7 is

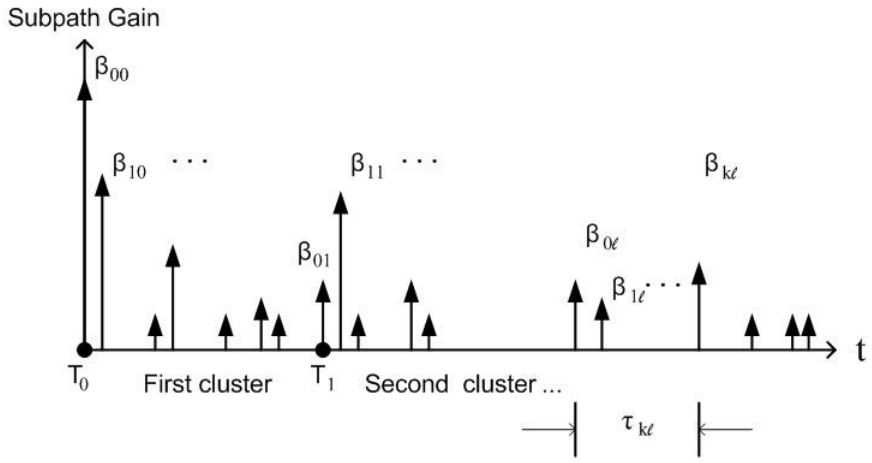

Figure 2.5: SVM channel impulse response

not an accurate representation of fig.2.5, so it is necessary to reformulate this equation into one expression less general and more precise, as can be seen in eq.2.11.

$$h(t) = \sum_{l=0}^{\infty}\sum_{k=0}^{\infty}\beta_{kl}e^{j\theta_{kl}}\delta(t - T_l - \tau_{kl}). \tag{2.11}$$

In fig.2.5, T_0 is the time arrival of first cluster, T_1 belongs to the second, and so on. τ_{kl} is the time interval from the beginning of the lth cluster to the klth ray arrival. The first cluster is the result of the main direct ray from the receiver to the transmitter, and the following subpaths (within this cluster) are due to the rebounds on the nearest walls. The additional clusters are cause by the reflections on the structure or internal elements of the test building, in this case two metallic doors of each room. Following the measurements

results, the cluster and ray arrival rates, Λ and λ respectively, can be expressed as a Poisson distributions associated with eq.2.8 for clusters and eq.2.9 for rays. The relationship between them are, approximately, $1/\Lambda \approx 60(1/\lambda)$.

Returning to eq.2.11, θ_{kl}'s are statistically independent uniform random variables over [0,2π). Additionally the β_{kl}'s are statistically independent positive random variables and their mean square value are

$$\overline{\beta_{kl}^2} = \overline{\beta_{00}^2} e^{-T_l/\Gamma} e^{-\tau_{kl}/\gamma}. \tag{2.12}$$

Here, Γ and γ are the power-delay time constants for the clusters and the rays respectively. The expected value of the ray power as a function of time, measured from the arrival point of the first ray of the first cluster, is given by

$$\overline{\beta^2(t)} = \overline{\beta_{00}^2} \sum_{l=0}^{L} e^{-T_l/\Gamma} e^{-(t-T_l)/\gamma} \cup (t - T_l), \tag{2.13}$$

when $\cup$ = 1 for t>0 and 0 for t<0. A graphic representation of eq.2.13 is shown in fig2.6. The red curves represent the ray power decay time function, $-\tau/\gamma$, and the green one,

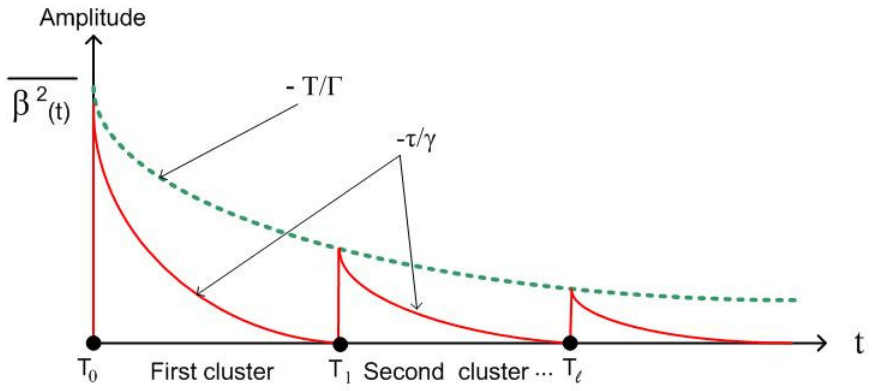

Figure 2.6: Exponentially decaying ray and cluster average powers

the cluster power decay time function, $-T/\Gamma$. The decreasing exponentially shape of each curve can be explained by the fact that the successive rays bounce along the building structure, making them suffer an average delay and average decibels of attenuation. On the other hand, the time interval from T0 to T1 represents the delay spread of the first

cluster. In the same way, the delay spread of the second one comes from T1 to T2 and so on.

Based on the results of the measurements, the SVM determine that the relationship between γ and Γ is such that $\Gamma \approx 3\gamma$. Anyway, this relationship may vary depending on the structure of the building.

Recent studies conducted in the *Institute of Radiofrequency and Microwave Engineering* from *Leibniz University of Hanover* [Vos08], have used this model to predict the channel behavior inside the Hanover Congress Center (HCC). These results are used in this thesis for comparison with the WINNER model, which is described further on. Before performing this analysis, the next subsection briefly describes the SCM and SCME channel models, which are the precursors of the WINNER channel model.

2.3 The SCM and SCME channel models

The spatial channel model, SCM, is also called geometric or ray based model, and it is based on stochastic modeling of scatters. Formerly, the tapped delay line, TDL, models have been designed for narrowband single input single output (SISO) systems. Moreover, they are applicable for link level testing only as a fixed parameter models, that is, they do not cover environment variability. Therefore, TDL models are not adequate for simulation and testing of broadband multi-antenna systems. Geometry-based stochastic channel models, GSCM, cover wide range of environments with random number parameters, supports different multi-antenna technologies such as beam forming and spatial multiplexing. The SMC models include simple TDL models for calibration purposes and GSCM for simulation purposes. Like Saleh-Valenzuela model, SMC also assumes that the rays, caused by the multipath propagation, reach the receiver grouped in clusters. The clusters indentified from measurements, are in general dispersed in angular and delay domains. However, in order to simplify the model while respecting the characteristics of the TDL models, SCM introduced clusters with zero delay spread, ZDSC. This feature does not appear in the Saleh-Valenzuela model in which cluster dispersion is quantified, as can be seen in fig.2.6.

The SCM model defines three environments: suburban macro, urban macro, and Urban micro, where urban micro is divided into two types of propagation, line of sight, LOS and non line of sight, NLOS. This model is defined for a 5MHz bandwidth CDMA system in the 2GHz band. Regarding the basic structure of the model, there are 120 discrete rays which are grouped into clusters of 20 subpaths each, i.e., there are 6 clusters at different delays. The angle and delay distributions of the clusters are randomized with exponential and Laplacian decay respectively. This model is valid for vertical and horizontal polarized antennas (transmitters and receivers) and it is assumed that the co-polarization power (vertical to vertical, VV, and horizontal to horizontal, HH) is equal at ray level.

The extension of SCM is called spatial channel model extended, SCME. SCME introduces cluster dispersion in delay domain (intra-cluster delay spread) to account for higher bandwidths and to reproduce the proper level of the frequency correlation. Despite this, and others additional features such as, 5GHz pathloss model, LOS and ricean k factor for all the scenarios, time-variant shadow fading and time-variant angles and delays, the SCME model has the same basic structure as the SCM model.

2.4 WINNER channel model

The WINNER channel model has been developed to provide a reliable tool for MIMO, SISO, MISO and SIMO radio channel estimations, covering frequencies in the range from $2-6$GHz and bandwidths up to 100MHz in different types of propagation environments. The first phase of the WINNER project was developed starting from SCM channel model and was quickly extended and improved in many aspects, based on the SCM extension, SCME. This version of WINNER is known as phase 2 of WINNER project and is the channel model used in this thesis. In the following subsections, the WINNER channel model and its application scenarios are described.

2.4.1 WINNER Channel model description

According to [Kyöb], the WINNER channel model is generated by following 3 main phases. The first phase begins by choosing the scenarios in which it is desirable the ap-

plication of this channel model. Before continuing, it is essential the knowledge of the parameters involved in the WINNER CIR measurements. There are two kinds of parameters defined in WINNER, large scale parameters and small scale parameters. Large scale parameters are:

- Delay spread. This parameter is explained in section 2.1.1.
- Angle of departure spread. It refers to the spread in the path's angles of departure, AoD's, that finally reach the receiver.
- Angle of arrival spread. It refers to the spread in the path's angles of arrival, AoA's, at the receiver antenna.
- Shadowing or shadow fading. It is a phenomenon that occurs when a mobile station (tranmitter or receiver) moves behind an obstructing object and experiences a significant reduction in signal power.
- Rician K-factor. It is defined as the radio of signal power in dominant component over the scattered power.

Small scale parameters are:

- The cross polarization power ratio, XPR. It is defined as the ratio between the power receiver by the antennas whose polarization is combined to the transmitted polarization and the power received by the antennas whose polarization is perpendicular to the transmitted. According to [Par] XPR can be expressed as

$$XPR = \frac{P_{combined}}{P_{perpendicular}} \tag{2.14}$$

- Since this model uses the ray and cluster concepts discussed above, all parameters associated with them are considered small-scale parameters like: number of cluster [1], cluster angle of departure spread, cluster angle of arrival spread, cluster shadowing and number of rays per cluster. This last parameter is fixed and equal for all WINNER scenarios.

[1] This parameter depends on the scenario chosen and the propagation condition.

- The auto-correlation and cross-correlation of the large scale parameters, are also small scale parameters.

This first phase ends with the measure of the small and large scale parameters over each scenario.Subsequently, this measures are stored in databasses. The second phase begins with the analysis and post-processing of the data measured. Statistical analysis of these post-processed data is carried out to obtain the probability density function, PDF, of each parameter. The third phase generates the channel model parameters by using the parameters PDF's. With all these parameters and with the antenna features, it is possible to obtain the channel impulse response matrix. The last part of the modelling process is to simulate each scenario and verify the results comparing with the data measured in the first phase.

In the WINNER model, unlike Saleh-Valenzuela model, each cluster is defined as a propagation path diffused in the space, and also, each one is characterized by the zero delay spread cluster (ZDSC) concept, first developed for the SCM model, as explained in the last section [2]. Moreover, the rays within each cluster have the same power and their number is fixed and equal for all WINNER scenarios, 20 rays per cluster. Fig.2.7 shows the generation of the ZDSC due to the multipath propagation.

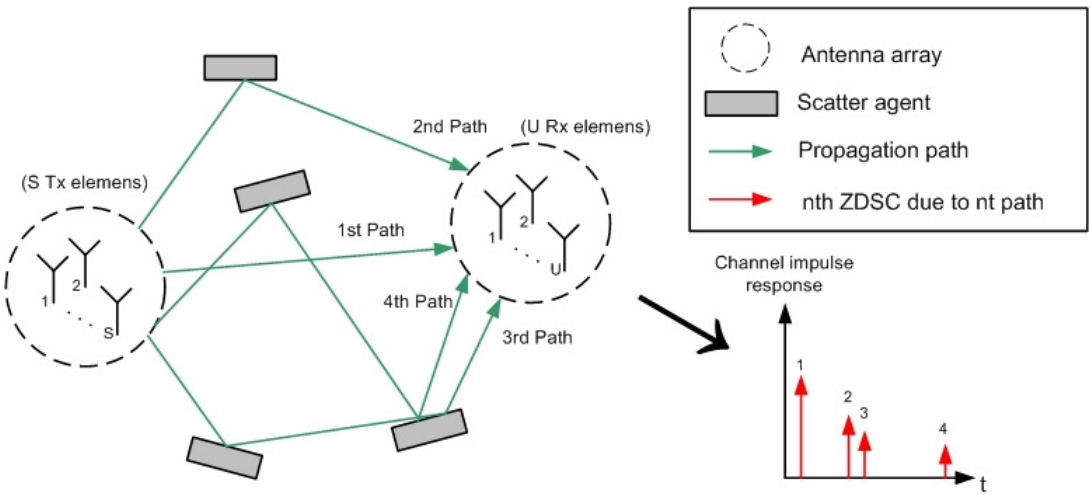

Figure 2.7: WINNER zero delay spread cluster (ZDSC) generation

[2]The WINNER model introduces the cluster delay dispersion for the two strongest clusters. The choice of the strongest clusters, depends on the scenario chosen.

In Fig.2.7, the scatters produce the different paths because of diffraction, reflection o scattering. The WINNER channel impulse response assumes that the first cluster reaches the receiver at $t = 0$. Each cluster corresponds to a path, and is defined by power amplitude, arrival time (delay), angle of departure (AoD) and angle of arrival (AoA). Both, the transmitter and receiver antennas, can be composed by several elements. Each element has its own radiation pattern which can be horizontal, vertical or both. Such antennas are called arrays. The channel impulse response from transmitter antenna element s to receiver antenna element u and for cluster n is, according to [Kyöb],

$$\begin{aligned} H_{u,s,n}(t;\tau) = \sum_{m=1}^{M} \begin{pmatrix} F_{rx,u,V}(\varphi_{n,m}) \\ F_{rx,u,V}(\varphi_{n,m}) \end{pmatrix}^{T} \begin{pmatrix} \alpha_{n,m,VV}\, \alpha_{n,m,VH} \\ \alpha_{n,m,HV}\, \alpha_{n,m,HH} \end{pmatrix} \begin{pmatrix} F_{tx,u,V}(\phi_{n,m}) \\ F_{tx,u,V}(\phi_{n,m}) \end{pmatrix} \\ \times exp(j2\pi\lambda_0^{-1}(\overline{\varphi}_{n,m} \cdot \overline{r}_{rx,u}))exp(j2\pi\lambda_0^{-1}(\overline{\phi}_{n,m} \cdot \overline{r}_{tx,u})) \\ \times exp(j2\phi\upsilon_{n,m}t)\delta(\tau - \tau_{n,m}) \end{aligned} \tag{2.15}$$

m is the ray index, where M is the total number of rays inside nth cluster. $F_{rx,u,V}$ and $F_{rx,u,H}$ are the antenna element u field patterns for vertical and horizontal polarizations, respectively. The location vector of each element, s and u, are $\overline{r}_{tx,s}$ and $\overline{r}_{rx,u}$. $\alpha_{n,m,VV}$ and $\alpha_{n,m,VH}$ are the complex gains of vertical-to-vertical and horizontal-to-vertical of ray n,m respectively. λ_0 is the wave length of the carrier frequency, $\overline{\phi}_{n,m}$ is AoD unit vector, $\overline{\varphi}_{n,m}$ is AoA unit vector. $\upsilon_{n,m}$ is the Doppler frequency component of ray n,m, whose delay is represented by $\tau_{n,m}$. The following subsection shows, more graphically, how the WINNER channel model operates in real environments.

2.4.2 Network layout and system level

Like stated in the introduction part of this section, the WINNER channel model enables MIMO, SISO, MISO and SIMO radio propagations. This characteristic leads in many complex propagation layouts with multiple stations, both receiving and transmitting. The WINNER model makes a distinction between two different types of stations: access point or base station, BS, and user terminal or mobile station, MS. Each BS, in turn, may be formed by several sectors or cells which provide their own coverage area. The connection between one MS and one BS's sector is called link.

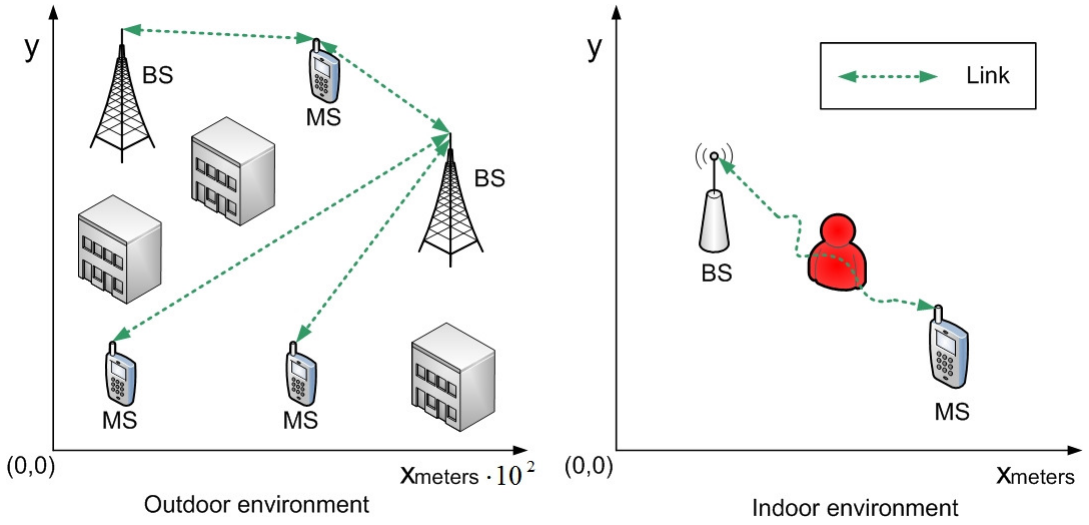

Figure 2.8: Examples of WINNER layouts for Outdoor and Indoor environments

As shown in fig.2.8, WINNER enables mono-link or multi-link channels. In multi-link situations spatial correlations of channel parameters are important. Correlation is caused by the effects of the same scatters in different links and affect, mainly, the large scale parameters. WINNER channel model only bear in mind the correlation in the case that two mobile stations were connected to the same BS's sector. This is called intra-cell correlation and follows a negative exponential dependence over the distance between both mobile stations.

Due to the movement of the stations, the WINNER channel impulse response is time-variant. This means that some realizations of impulse response are calculated in different time moments until the connection ends or the station stops. The WINNER model defines segments as the portions of the way that travels one station, in which the large scale parameters, velocity and direction of the station are practically constant. The size of these sectors depends on the environment and can be, at most, a few meters. For example, if one MS crosses a urban sector composed by some BS's, the path traveled by the MS is divided into subsequent and equal segments with space length between them equal to the same size of the segments. In order to support "smooth" model evolution in time, transitions from segment to segment are carried out by replacing clusters of the "old"

segment by clusters of the ”new” segment, one by one, by linearly decreasing-increasing their powers.

2.4.3 Propagation scenarios

The parameters used by the WINNER channel model are obtained from channel measurements in different environments. These environments, in which measurements are conducted to observe radio-channel characteristics, are called propagation scenarios. For each scenario measured, data is analyzed and complemented with results from other researches to obtain scenario-specific parameters. The WINNER model has been developed for 18 scenarios divided into three categories: local area, metropolitan area and wide area. In certain scenarios, WINNER is able to simulate situations like:

- Handover. This situation is characterized by a MS moving from the coverage area of one BS to the coverage area of another BS.
- Multi-user. Is the same situation above but here the MS receives data from multiple BS simultaneously.
- Multihop. In multihop situation the data can take a route from MS to BS, over one or more successive mobile stations.
- Relaying. Relaying networks employ another level of network stations, the relays, which depending on the specific layout, might offer more or less functionality to distribute traffic intelligently.

From all the available WINNER scenarios, the relevant ones for the PWMS application under study in this thesis are described next:

- A1. Indoor office. In this scenario, base stations are assumed to be in the corridor and the mobile stations are in the corridors or rooms, thus LOS case is corridor-to-corridor and NLOS case is corridor-to-room.
- B3. Indoor hotspot. Scenario B3 represents the propagation conditions pertinent to operation in a typical indoor hotspot, with wide, but non-ubiquitous coverage and low mobility (0-5 km/h). Traffic of high density would be expected in such

scenarios, as for example, conference halls, factories, train stations and airports. These indoor environments are characterized by larger open spaces, where ranges between a BS and a MS or between two MS can be significant. Typical dimensions of such areas could range from 20 m x 20 m up to more than 100 m in length and width and up to 20 m in height.

2.5 COST 259/273 channel models

"COST" is an abbreviation for European cooperation in the field of scientific and technical research. COST developed channel models that include directional characteristics of radio propagation. These models are suitable for MIMO channel simulations. Focused in wireless communications, the two main models developed by COST are COST 259 and COST 273.

2.5.1 COST 259

COST 259 is a channel model that models the delay and angle dispersion of a mobile station and base station. The model also takes into account the relationship between BS-MS distance, delay spread, angular spread [3], and other parameters. COST 259 is defined for 13 different scenarios including indoor scenarios like rooms or big halls. The radio links between one BS and one MS are described by external parameters and global parameters. The external parameters are, for example, BS position and height, frequency, type of scenario etc. The global parameters describe the instantaneous channel behavior. They are determined geometrical and stochastically. The scatters that produce clusters are located geometrically inside a cell (macro, micro or pico). Other global parameters like angular spread, delay spread, and shadowing are determined stochastically. From the external and global parameters, COST 259 calculates the relative delays and mean angles of different clusters that make up the channel impulse response.

[3] This parameter represents the range of all angles of arrival and departure

COST 259 can handle the continuous movement of the MS over several propagation environments, but one of its major restrictions is that the scatters are assumed to be stationary, that is, they are fixed. This means that it excludes certain environments like, for example, indoor scenarios with people moving inside.

2.5.2 COST 273

COST 273 is an evolution of COST 259. It shares with 259 most of its main features, but differs in several key aspects: There are new radio environments defined that permit new simulation applications for MIMO channels. The global parameters have been updated based in new measurement campaigns. COST 273 describes each cluster via two twin clusters, one that represents the cluster as seen by the MS and one as it is seen by the BS. The two cluster representations are linked via one parameter called stochastic cluster link delay. This channel model does not solve the restriction of fixed scatters so both models are limited for PWMS applications.

2.6 The IEEE 802.11 TGn channel model

The TGn channel model was developed for MIMO channels in the 2GHz and 5GHz bands. TGn is defined for indoor scenarios like small and large offices, residential homes, and open spaces. These scenarios are divided into six categories, and in all of them, are considered LOS and NLOS cases.

The channel impulse response is defined as a sum of clusters. Based on measured data the numbers of clusters varies from 2 to 6 depending on the environment chosen. Each cluster is formed by 18 rays as maximum, separated by at least 10 nanoseconds. To each ray is assigned a direction of arrival, DoA, and a direction of departure, DoD.

TGn model permits CIR's variations, emulating, in contrast to COST 259/273, the movement of the scatters. This feature makes TGn model more suitable for the PWMS application of this thesis than COST 259/273.

3 WINNER implementation

As mentioned several times in previous chapters, one of the main tasks of this thesis is to compare the channel impulse response, obtained from real measurements and analyzed with the Saleh-Valenzuela model, with the channel impulse response simulated with the WINNER model. In both cases, for the same PWMS application, that is, the application scenarios, in which both models have been simulated, should be as similar as possible and based, in this case, on the general structure of the Hannover Congress Center hall. One of the channel impulse responses that are going to be compared, corresponding with the Saleh-Valenzuela model, was obtained in a previous research [Vos08] in which, channel measurements were taken inside the HCC hall and processed using Matlab. The impulse response was obtained by modelling this processed data, based on Saleh-Valenzuela model theory explained in the last chapter. Results from [Vos08] are presented and analyzed in chapter 4 of this thesis. The second channel impulse response to compare, based on the WINNER model, is obtained during this report.

The implementation of the WINNER channel impulse response is carried out by working with Matlab using the WINNER Matlab code provided by [Narb]. The first step is to go deepen in this code to discover the design possibilities the WINNER model offers and, subsequently, and according to with these possibilities, define a simulation setup as close as possible to that used in the Saleh-Valenzuela channel model. This setup includes an environment design (which should be as similar as possible to the HCC hall) as well as the transmitter and receiver station descriptions. The following subsections show an overview of the WINNER Matlab code and their setup options. It also explores the changes in the code that are required to build the desired simulation environment.

3.1 Winner Matlab code

The WINNER channel model Matlab code allows to generate a multidimensional channel matrix, H, that contains the time-variant channel impulse responses, CIR's, between all transmitter and receiver antenna combinations of MIMO system. The code consists of 42 files and 3 application examples. Each Matlab file has its own function and relevance. In this way, there are secondary files that only support other more important whose output defines key parts of a communication system such as, the antennas configuration, the environment description or the channel model simulation parameters. Some of the 42 files provided by WINNER are not used for calculate the channel impulse response. They are description files or auxiliary files for specific cases. For example, *pathloss.m* calculates the path losses of the scenario chosen. This file is independent of *wim.m*[4],and is not used to obtain the channel impulse response, making it not relevant for this thesis. Other independent files like, for example, the application examples are not relevant as well. The list with all the files is shown in [Narb]. This chapter is focused, only, on the files that are used to obtain the WINNER channel impulse response. Fig.3.1 shows the relationship between these files using a hierarchy tree. In this way, the grey blocks represents the main files used by WINNER for calculate the impulse response. Each file depends in turn on other secondary files framed by an ellipse and these secondary files also depend on other functions. For example, both *AntennaArray.m* and *wim.m* use *AntennaResponse.m* indirectly in the first case and directly in the second.

The core code-file of WINNER is *wim.m*, which exports a channel impulse response matrix for a specific layout. *wim.m* inputs, are the communication link description provided by *layoutparset.m* and the simulation conditions described in *wimparset.m*. In turn, *layoutparset.m* uses the antenna characteristics described in *AntennaArray.m*. Other files like *layoutparset.m*, *wimparset.m* and *AntennaArray.m* can be considered as a pre processing phase. This means that, before calculating the WINNER CIR using *wim.m*, it is necessary to set the parameters provided by these files.

The basic operation of *wim.m* goes as follows: *wim.m* picks up the information from the pre processing phase. This information includes the antenna characteristics, the layout

[4]This is the main WINNER Matlab code file.

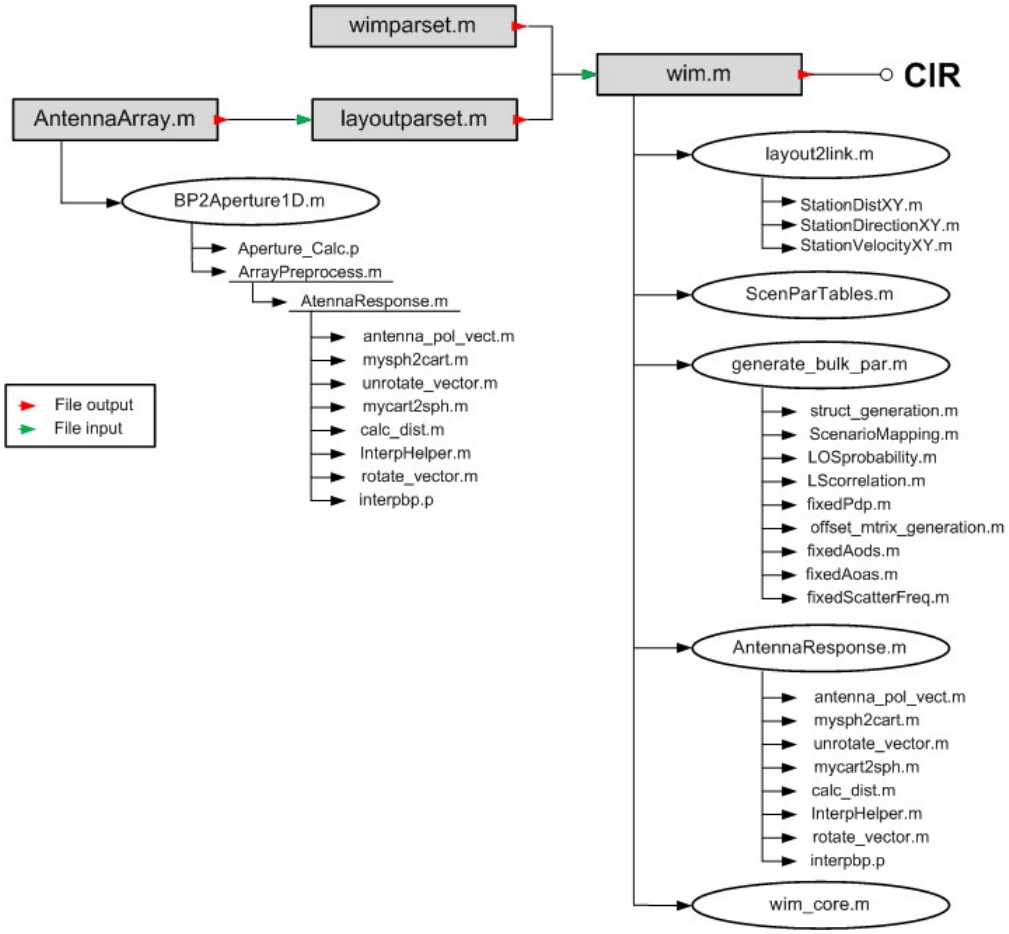

Figure 3.1: WINNER Matlab files relationship diagram.

parameters and the simulation parameters. Inside *wim.m*, there are two main parts, the random user parameter generation and the channel impulse response computation. The first part is performed by the file *generate_bulk_par.m*. This file generates randomly the small and large scale parameters of the WINNER model. *wim.m* ends its operation by generating the channel impulse response matrix from the parameters provided by the input arguments and *generate_bulk_par.m* output. This second part is performed by *wim_core.m*, which computes one CIR matrix for each one of all communication links. The channel impulse response calculated is formed by N clusters (depending on the scenario chosen) and M rays (always 20) within each cluster. The following subsections describe the pre

processing phase files and go more into details in the description of the operation of *wim.m*.

3.1.1 Antenna model for WINNER channel simulations

The WINNER model supports multi-element antennas called antenna arrays. Each antenna array is placed and oriented anywhere with respect the global coordinate system, GCS. Antenna arrays have also its own coordinate system called array coordinate system, ACS, which is used to locate the elements of each antenna array. Every mobile station or base station used in WINNER simulations can use different antenna arrays in which the radiation pattern of each element can be independently defined. *AntennaArray.m* is the file responsible for building the antenna arrays. The output of this file is a Matlab structure that contains the description of the desired antenna, and it is one of the inputs of *layoutparset.m*. This structure contains the following information: the antenna name, the antenna position and rotation with respect to the GCS, the position and rotation of each antenna element with respect to the ACS and the radiation pattern features. The *AntennaArray.m* input parameters are the antenna geometry and the antenna radiation pattern [5]. These parameters can be set manually or using default values. If the default values are chosen, one antenna with only one element is created in the center of the ACS. This antenna presents no rotation, an isotropic field pattern and vertical polarization.

Antenna geometry

The WINNER channel model works with two kinds of antenna array shapes: uniform circular array (UCA), in which the elements are placed following a circle, and uniform linear array (ULA), in which the elements are located following a straight line. *AntennaArray.m* allows to specify the type of array geometry, the number of elements, the distance between them and their position and rotation within each antenna array.

Antenna radiation pattern

The WINNER channel model allows working with 2 dimensional or 3 dimensional antenna radiation patterns. For 3D patterns, it is necessary to define azimuth and elevation

[5] Field pattern.

vectors, whereas that only azimuth or elevation vector is necessary for 2D radiation patterns. The number of samples in each vector determines the resolution of radiation pattern. The input radiation pattern defined by the user must be a 4D Matlab matrix due to format restrictions. The first dimension is the number of elements, the second dimension is the polarization type, the third dimension is the number of equidistant field pattern samples taken over elevation angle and the fourth dimension is the number of equidistant field pattern samples taken over azimuth angle. This 4D matrix can be understood as a 2D matrix for each elevation and azimuth value. The number of rows of this 2D matrix must be the same as the number of elements inside the antenna array, and the columns represent the antennas polarizations, vertical and horizontal. The first column corresponds to vertical polarization and the second one to horizontal polarization. In the case of 2D radiation patterns, it is necessary to choose a polarization. If, for example, horizontal polarization is chosen, the column corresponding with the vertical polarization is filled with zeros, resulting that the size of the second dimension of the 4D matrix is always 2. The next equation represents the general expression of the WINNER antenna field pattern.

$$FP_{ij} = \begin{pmatrix} a(ij)_{11} & a(ij)_{12} \\ a(ij)_{21} & a(ij)_{22} \\ \vdots & \vdots \\ a(ij)_{n1} & a(ij)_{n2} \end{pmatrix} \tag{3.1}$$

FP_{ij} is the field pattern in the ith azimuth angle and jth elevation angle of an antenna which is composed of n elements. For example, for a single antenna with 3D isotropic field pattern and 360 samples in azimuth and 180 in elevation, the size of each dimension of the 4D matrix will be 1, 2, 180 and 360 respectively. Eq.3.2 shows the mathematical expression of this example whereas that eq.3.3 represents, for the same angles of azimuth and elevation, a 2D isotropic antenna with horizontal polarization.

$$FP1_{ij} = \begin{pmatrix} 1 & 1 \end{pmatrix} \qquad for 1 \leq i \leq 360; 1 \leq j \leq 180 \tag{3.2}$$

$$FP2_{ij} = \begin{pmatrix} 0 & 1 \end{pmatrix} \qquad for 1 \leq i \leq 360; 1 \leq j \leq 180 \tag{3.3}$$

Assuming that $FP1$ is the variable that contains the radiation pattern of the first example, $FP1(1,2,100,200)$ returns a number that correspond with the radiation power level of the horizontal polarization of the 100th sample of elevation and 200th sample of azimuth, $FP1(1,2,100,200) = 1$.

This 4D matrix that describes the radiation pattern requires high amounts of memory storage, so WINNER transforms it into other less complex but enough representative format. This format is called the Effective Aperture Distribution Function, EADF. According to [Nara][Lan], EADF achieves a high data compression, allowing WINNER code to reduce the number of samples needed to fully describe a field pattern. Taking the last example where the samples required were 180x360, the number of samples required in EADF to have a good resolution of the field pattern is around 40x60. EADF is the 2D-Fourier transform of the original field pattern introduced by the user. The next equations show the mathematical relationship between field pattern, FP, and the EADF, represented by G in eq 3.4.

$$FP(\varphi,\theta) = d_{b1}(\theta) \cdot G \cdot d_{b2}(\varphi), \tag{3.4}$$

where

$$\begin{aligned} d_{b1}(\theta) &= e^{j\theta\mu_1^T} \\ d_{b2}(\varphi) &= e^{j\varphi\mu_2^T}, \end{aligned} \tag{3.5}$$

and

$$\begin{aligned} \mu_1 &= \left[\frac{-(L_1-1)}{2}, \ldots \frac{(L_1-1)}{2}\right]^T \\ \mu_2 &= \left[\frac{-(L_2-1)}{2}, \ldots \frac{(L_2-1)}{2}\right]^T \end{aligned} \tag{3.6}$$

θ refers to azimuth and φ refers to elevation. L_1 and L_2 are the new number of samples required. Fig.3.2 shows a graphical example of the EADF of a 3D isotropic antenna field pattern. Since the fig.3.2 a) and fig.3.2 b) are equivalent representations of the antenna radiation pattern, fig.3.2 b) is the most efficient representation because it requires less information that fig.3.2 a) to represent the same antenna field pattern.

A diagram of the construction process of an antenna using WINNER Matlab code is presented in fig.3.3.

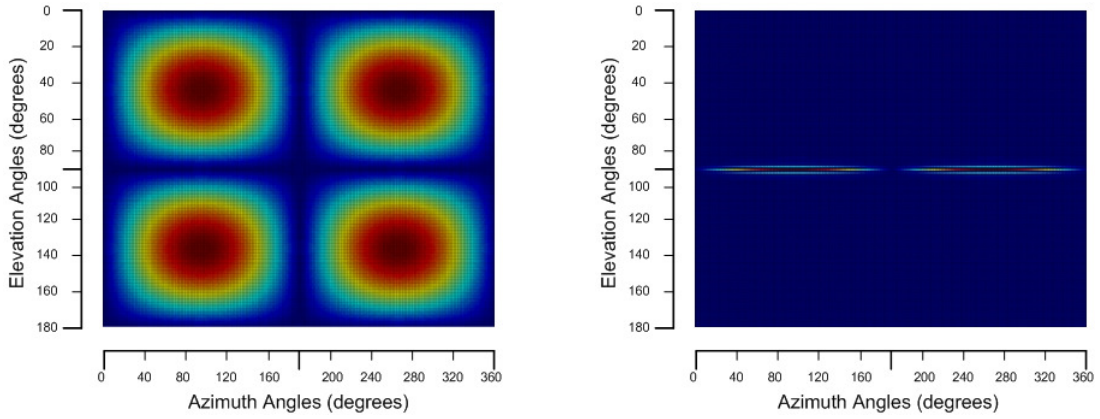

Figure 3.2: (a) 3D isotropic antenna field pattern; (b) EADF

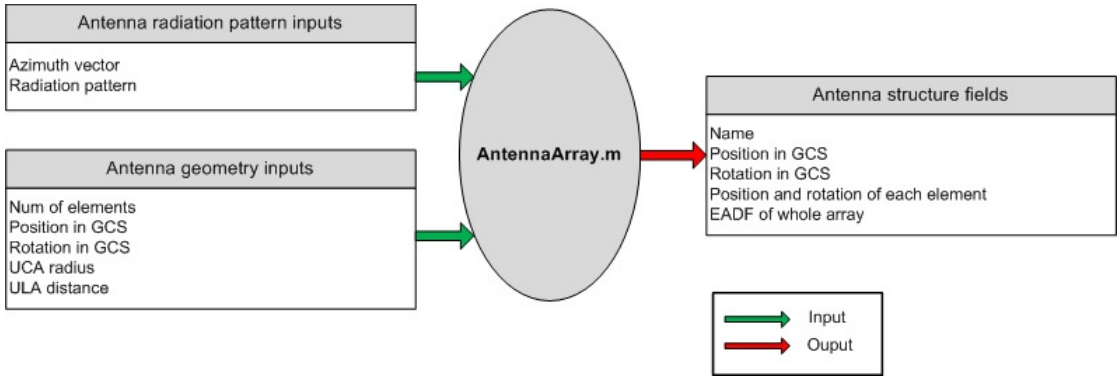

Figure 3.3: Antenna array construction process diagram

3.1.2 Network layout parameters

The definition of layout parameters is another task inside the pre processing phase. The Matlab file responsible for performing this function is *layoutparset.m*. It defines the position of the terminal stations [6]. Also it assigns the antenna array for each station and establishes the communication links between them. Before executing this function, it is necessary to define their input parameters. These parameters are listed below:

[6]Mobile station, MS, and base station, BS.

- Antenna arrays. This input consists of a vector where each element is an antenna array structure created by *AntennaArray.m*
- Mobile stations. This input is a vector whose size depends on the number of mobile stations required for the simulations. The value of each vector element is a number that corresponds with one of the index of the antenna array vector. In this way, it is possible to assign one specific type of antenna array to each mobile station.
- Base stations. This input defines the number of base stations and the number of sectors of each one in case of multi-cell network. Also, it sets the type of antenna array for each station and sector. This input is a vector whose size determines the number of base stations. Each vector element is, in turn, another vector with only one row whose length defines the number of sectors of each base station. To assign the type of antenna to each sector, this input works the same way as mobile stations, that is, the values of the vector elements (BS sectors) correspond to one of the index of the antenna array vector, depending on the desired antenna type.
- Maximum radius of the simulation area. It is the maximum value for x and y axis of the cartesian GCS used for simulating an specific case. The default value is 500 meters. The size of the simulation area is generated randomly, never exceeding the maximum radius.
- Number of links. This parameter specifies the number of communication links between all terminals under simulation. The location of such links is done, as it is mentioned below, randomly. Typically, the number of links is represented by the letter K.

The output of *layoutparset*, called *layoutpar*, is a Matlab structure consisting of semi-random generated network layout parameters. The location in GCS of terminal stations, the assignment of their antenna arrays, and the number of links between them are set manually, but the links between different stations are generated randomly. As seen in fig.3.1, this output is, in turn, a *wim.m* input. The parameters of *layoutpar* are listed below:

- *Stations*. This is a Matlab structure that shows the information of the stations involved on simulations. This information includes the name, position, rotation and

velocity of each station. Position, rotation and velocity are set using cartesian coordinates in GCS. This parameter also includes the position and location of the antenna elements of each station, and its radiation pattern.

- *NofSect*. This parameter defines the number of sectors of each BS. *NofSect* is a vector whose size depends on the number of base stations.
- *Pairing*. It is a 2xK matrix that contains the indices of stations that constitute the Kth link. K is the number of links that are set in the *layoutparset.m* input.
- *ScenarioVector*. The Matlab file *ScenarioMapping.m* provides an identification value for each WINNER scenario. For example, the identification value of scenario A1 is 1 and for scenario B3 is 5. ScenarioVector is a 1xK vector where the value of each vector element corresponds with one scenario identification value. Therefore, each link is simulated under the features of the scenario chosen.
- *PropagConditionVector*. This parameter is also a 1xK vector and determines the propagation condition of each communication link, LOS or NLOS. The two possible values of vector elements are 1 for LOS and 0 for NLOS.
- *NumFloors*. This parameter is only used in A2 and B4 scenarios and defines the number of floor in which the BS and MS are located.
- *NumPenetratedFloors*. This parameter is only used for *pathloss.m*. It defines the number of floors between one BS and one MS when they are located inside a building in the A1 scenario.
- *Dist*1. Used for *pathloss.m*, is the distance from BS to the "last line-of-sight point", typically street crossing.
- *StreetWidth*. Also used for *pathloss.m*, determines the average width of the streets in B1 and B2 scenarios. It is the same for all links.

As in the previous subsection, fig.3.4 shows a summary chart of the main structure of this file.

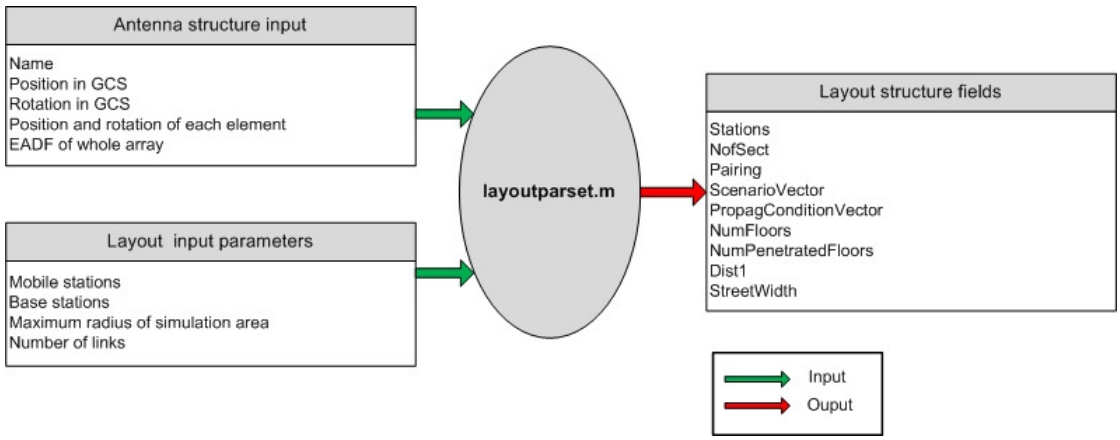

Figure 3.4: Layout parameters diagram

3.1.3 General simulation parameters

As well as *AntennaArray.m* and *layoutparset.m*, *wimparset.m* also belongs to the pre processing phase. This Matlab file usually runs without setting input parameters, so the output structure generated by *wimparset.m* contains the default values of the general simulation parameters. Modifications in these parameters must be done over the structure generated, and before executing *wim.m*. Global simulation parameters can be classified into two major groups: parameters defining model and simulation control parameters.

Parameters defining model. In this group changes in the parameters cause different model behavior.

- *CenterFrequency*. This is the carrier center frequency. The *CenterFrequency* parameter in WINNER model is only relevant for estimating the time sample interval and the path losses. The WINNER model path losses are based on measurements that are mainly conducted in 2 and 5GHz and are valid for the range of $2-6$GHz. Therefore, for path loss calculations the *CenterFrequency* must to set between 2 and 6. The default value is 5.25GHz.
- *Range*. This parameter is used for scenario B5b when *pathloss.m* is executed. By default this parameter is inactive.

- *IntraClusterDsUsed*. As discussed and explained in chapter 2, one of the WINNER cluster features is that the delay spread of each cluster is zero. However and according to [Vos08], the WINNER channel model is able to simulate the cluster dispersion, through the division of the two strongest clusters into three sub-clusters with zero delay spread. The delays of these sub-clusters are fixed always with the same value, 0, 5 and 10 nanoseconds. The 20 rays belonging to the cluster that has been divided, are distributed among the three sub-cluster according to the table 3.1 obtained from [Kyöb]. This table also shows the fixed power level of the rays within each sub-cluster and the sub-cluster delays. The cluster subdivision does not increase the total number of paths. If *ItraClusterDsUsed* is enabled,'yes', WINNER spread in delay the two strongest clusters. In case of 'no', cluster delay spread effect is not simulated.

sub-cluster	mapping to rays	power	sub-cluster delay (ns)
1	1,2,3,4,5,6,7,8,19,20	10/20	0
2	9,10,11,12,17,18	6/20	5
3	13,14,15,16	4/20	10

Table 3.1: Sub-cluster information for intra cluster delay spread clusters

- *NumSubPathsPerPath*. This parameter determines the number of rays inside each cluster. Its value is fixed, 20.

- *FixedPdpUsed*. WINNER provides cluster delay line (CDL) models for all scenarios. CDL models have been generated from the corresponding generic models by selecting typical values from a set of random channel realizations. The CDL models fix the value of cluster delay time and power, the angle of arrival, the angle of departure, the power of rays within each cluster, the cluster azimuth spread of departure, the cluster azimuth spread of arrival, and the cross polarization, XPR. In [Kyöb] the tables with all this parameters for all scenarios are presented. If *FixedPdpUsed* is enabled, 'yes', the power and delay parameters are not drawn randomly, but taken from the CDL parameter tables. In the default mode, 'no', the parameters are random variables generated by *generate_bulk_par.m*.

- *FixedAnglesUsed*. If *FixedAnglesUsed* is enabled, 'yes', the angle parameters are not drawn randomly, but taken from the CDL parameter tables. In the default mode, 'no', the parameters are random variables generated by *generate_bulk_par.m*.
- *PolarisedArrays*. If *PolarisedArrays* is 'yes', single channel coefficient of impulse response turns to 2x2 coefficient matrix, with elements [VV VH;HV HH].Where V stands for vertical polarisation and H for horizontal. The default value is 'no'.
- *TimeEvolution*. If TimeEvolution is enabled, 'yes', the transition between adjacent channel segments (see subsection 2.4.2) is enabled making the model "smooth" in time evolution. The default value is 'no'.
- *PathLossModel*. This parameter sets the name of the path loss function used. The default value is 'pathloss'.
- *PathLossOption*. This parameter sets the type of material of which the walls of the building are made for A1 NLOS path loss calculation. There are two kind of NLOS path. One from corridor to room, CR, and the other one comes from room to room, RR. There are, also, two kind of wall material, heavy and light. The default value is 'CR_light'.

Simulation control parameters. These parameters control sampling in time and delay, parameter initialization mode, and format of output parameters.

- *NumTimeSamples*. The default value for the number of time samples is 100. As discussed below, this parameter determines the size of the CIR matrix.
- *SampleDensity*. This parameter is the number of time samples per half wavelength and its default value is 2. *SampleDensity*, *CenterFrequency* and the velocity of the mobile station, MS Velocity, determine the time sample interval based on the following formula.

$$\Delta T = \frac{\lambda}{2(v_{MS} \times sd)} \tag{3.7}$$

  ΔT is the time sample interval, λ is the wavelength, v_{MS} is the velocity of the mobile station and *sd* is the parameter *SampleDensity*.
- *UniformTimeSampling*. If *UniformTimeSampling* is 'yes' all links will be sampled at simultaneous time instants. In this case, the time sample interval is the same

for all links and it is calculated by replacing MsVelocity with its maximum, where the maximum is over all links. The default value is 'no'.

- *DelaySamplingInterval*. *DelaySamplingInterval* determines the sampling grid in the delay domain. All path delays are rounded to the nearest grid point. It can also be set to zero. The default value is 5 nano seconds.
- *PathLossModelUsed*. This parameter is relevant only in the case that path losses are calculated. If *PathLossModelUsed* is 'no' the path losses are still computed for each link but they are not multiplied into the channel impulse response matrices. If 'yes', path loss is multiplied to channel impulse response matrices. Its default value is 'no'.
- *UseManualPropCondition*. If this parameter is set to 'yes', the propagation condition, LOS or NLOS, is set manually by modifying the parameter *PropagConditionVector* of the function *layoutparset.m*. In case of 'no', the propagation condition is drawn from LOS probabilities presented in [Kyöb](table 4.7).
- *ShadowingModelUsed*. When *ShadowingModelUsed* is 'no' the shadowing coefficients are still computed for each link but they are not multiplied into the channel impulse response matrices. If it is set to 'yes', shadowing is multiplied to channel impulse response matrices. The default value is 'no'.
- *RandomSeed*. This parameter sets random seeds for Matlab random number generators. The default value is an empty Matlab array, [].
- *end_time*. This parameter determines the observation end time for B5 scenarios. Its default value is 1 second.

Fig.3.5 shows the *wimparset.m* file diagram.

3.1.4 Channel impulse response generation

As mentioned earlier in subsection 3.1, the WINNER Matlab code file that calculates the channel impulse response matrix is *wim.m*. The inputs of this file are the outputs of *layoutparset.m* and *wimparset.m* described before. There is, also, another input usually

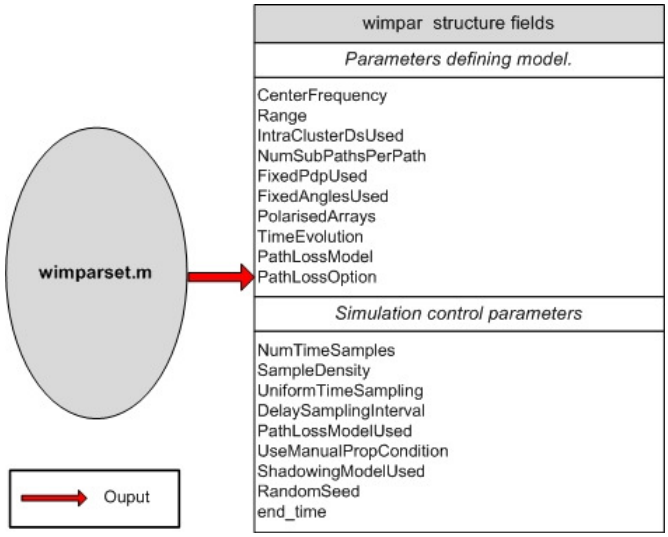

Figure 3.5: General simulation parameters diagram

called *initvalues*. This optional argument contains the propagation channel parameters. If *initvalues* are included in the input arguments of *wim.m*, *wim.m*, along its execution, does not use the *generate_bulk_par.m* file. This mean that the propagation channel parameters are not randomly generated, but are supplied by *initvalues*. Including *initvalues* as an input argument is recommended when *wim.m* is executed recursively, or if it is used for testing purposes. The propagation parameters provided by *initvalues* are listed below.

- Cluster delays. It is a KxN matrix that contains the time arrival of each cluster, where K is the number of links and N is the number of clusters.
- Power of rays. This parameter is the power level values of each ray within each cluster. It is represented by a 3D matrix; KxNxM. M represents the number of rays within each cluster.
- Angle of departure of rays. This parameter has the same format that previous parameter, KxNxM.
- Angle of arrival of rays. This parameter has the same format that previous parameter, KxNxM.

- Phase of rays. This parameter is based on the antennas dual polarization, vertical and horizontal. The ray phase from one antenna to another follows 4 possible paths, vertical to vertical, vertical to horizontal, horizontal to vertical and horizontal to horizontal. Hence, the format of this parameter is a Kx4xNxM matrix.
- Path losses. This parameter contains the path loss of each communication link, and its format is a Kx1 vector calculated by *pathloss.m* file.
- Index of two strongest clusters. This is a Kx2 matrix that determines the two strongest clusters for each link.

The first task of the function *wim.m* consists on generating the large and small scale propagation parameters. In the case that *initvalues* was not an input variable, the Matlab file that generates these parameters is *generate_bulk_par.m*. This function returns a Matlab structure that contains all the propagation parameters required for calculating the channel impulse response matrix in the second part of the *wim.m* process. The inputs of *generate_bulk_par.m* are *wimpar*, *linkpar* and *fixpar*. The first one is the *wimparset.m* output structure. *linkpar* is generated by *layout2link.m* based on *layoutpar*. This is a structure that has the same parameters as *layoutpar*, but adding some more. These new parameters are focused on link level layout, unlike the *layoutpar* parameters which were more focused on system layout level. Fig 3.6 is an example of WINNER link level layout situation. The link level parameters contain the information about the position, rota-

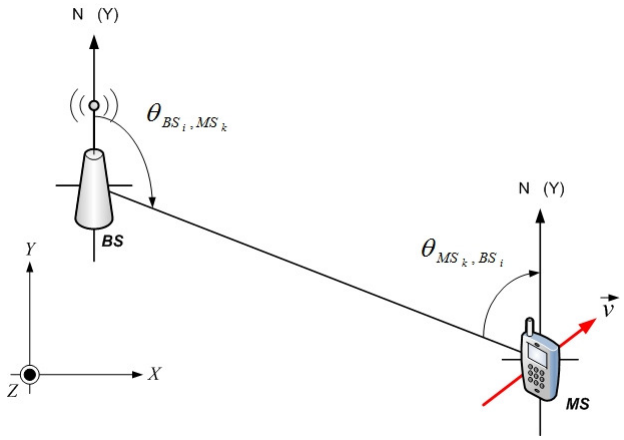

Figure 3.6: Link level situation between BS and MS

tion, movement and size of the interacting pair of stations of a radiolink. The parameter *MsBsDistance* is a $1xK$ vector that contains, for all links, the distance between one base station and one mobile station belonging to the same link. To calculate this parameter, the formula used is the Euclidean distance formula.

$$d_{BS_i,MS_k} = \sqrt{(x_{BS_i} - x_{MS_k})^2 + (y_{BS_i} - y_{MS_k})^2}. \tag{3.8}$$

x_{BS_i} and x_{MS_k} are the x position in GCS of the ith base station and the kth mobile station respectively. In the same way, y_{BS_i} and y_{MS_k} are the y position in GCS of the ith base station and the kth mobile station.

BsHeight and *MsHeight* are a 1xK vector that defines the BS and MS height respectively from the groud level. *BsHeight* and *MsHeight* are derived from the BS and MS station z value in GCS. These parameters are defined in meters. The rotation information of the stations is determined by *ThetaBs*, θ_{BS}, and *ThetaMs*, θ_{MS} (see fig 3.6). Both *ThetaBs* and *ThetaMs* are represented in radians and calculated following this expression:

$$\theta_{BS_i,MS_k} = -arctan\left(\frac{y_{MS_k} - y_{BS_i}}{x_{MS_k} - x_{BS_i}}\right) + 90^\circ. \tag{3.9}$$

MsVelocity is the *linkpar* parameter that contains the velocity of the MS station in meters per second, m/s, and it is derived from the station velocity cartesian coordinates established in *layoutparset.m*, from which also derives the direction (in radians) of the mobile station, *MSDirection*.

Returning to *generate_bulk_par.m* input parameters, the last one is *fixpar*. This parameter is the output of the Matlab file *ScenParTables.m*. This file contains, and loads into *fixpar*, the scenario specific parameter values of WINNER generic channel model, see [Kyöb]. The *generate_bulk_par.m* output structure is generated from inputs explained above, and using the WINNER Matlab files related with this file (see fig.3.1). This structure provides the following parameters: the power level of each cluster; the angles of arrival, AoA's, the angles of departure, AoD's and the phase of the rays within each cluster; the rician K-factors for all links, called K-factors; the final phases of LOS paths called Phi_loss; the path losses; shadow fading; the distance between BS and MS, both in the same link; the correlation coefficients for large scale parameters called sigmas, and the

cluster arrival time, that is, the cluster delays [7]. In the case that *wimpar.PolarisedArrays* is enabled, *generate_bulk_par.m* also returns the horizontal and vertical cross-polarization values, xprV for vertical polarization and xprH for horizontal polarization.

The last task done by *wim.m* before generating the channel impulse response matrix is to obtain the antenna responses using *AntennaResponse.m* file. This file provides the gain of each antenna array. After this, *wim.m* is ready to calculate the channel impulse response. For this purpose *wim.m* executes the *wim_core.m* file. This file uses as inputs *wimpar*, *linkpar*, the propagation parameters given by *genrate_bulk_par.m* and the gain of the antenna arrays provided by *AntennaResponse.m*. The CIR format is a Matlab cell that contains a 4D matrix for each link, that is, K 4D matrices. Each matrix represents the channel impulse response of one link. The general expression of the CIR matrix is presented in the next equation

$$CIR_{ij} = \begin{pmatrix} a(ij)_{11} & a(ij)_{12} & \cdots & a(ij)_{1m} \\ a(ij)_{21} & a(ij)_{22} & \cdots & a(ij)_{2m} \\ \vdots & \vdots & \ddots & \vdots \\ a(ij)_{n1} & a(ij)_{n2} & \cdots & a(ij)_{nm} \end{pmatrix} \tag{3.10}$$

Eq.3.10 format is very similar to the format of eq.3.1, but, in this case i is the cluster number and j represents the jth time sample. The number of MS antenna elements is n and m is the number of the antenna elements of the BS. Each coefficient, a, is a complex number that contains the phase and amplitude information of the impulse response between different elements of each antenna belonging to a link. In summary, there is a NxM matrix per cluster and per time sample.

For example, if one link with a BS antenna with 4 elements and a MS antenna with 2 elements, is simulated inside A1 scenario (12 clusters) and during 100 time samples, WINNER code generates 1200 matrices whose size is 2x4.

$$CIR_{ij} = \begin{pmatrix} a(ij)_{11} & a(ij)_{12} & a(ij)_{13} & a(ij)_{14} \\ a(ij)_{21} & a(ij)_{22} & a(ij)_{23} & a(ij)_{24} \end{pmatrix} \qquad for 1 \leq i \leq 12; 1 \leq j \leq 100 \tag{3.11}$$

[7] When $FixedPdpUsed$ and $FixedAnglesUsed$ are enabled the large scale parameters are not generated by *generate_bulk_par.m*.

In this example $CIR(1,3,7,50)$ returns the complex number that represents the amplitude and phase of the 7th cluster in the 50th time sample of the impulse response between the first element of MS antenna and the 3rd element of BS antenna.

Moreover, *wim.m* has two other outputs. The first one is a vector that contains the time arrival of each cluster, and the second one is a structure composed by all the parameters generated by *generate_bulk_parameters*. Fig.3.8 shows a complete diagram of *wim.m* operation.

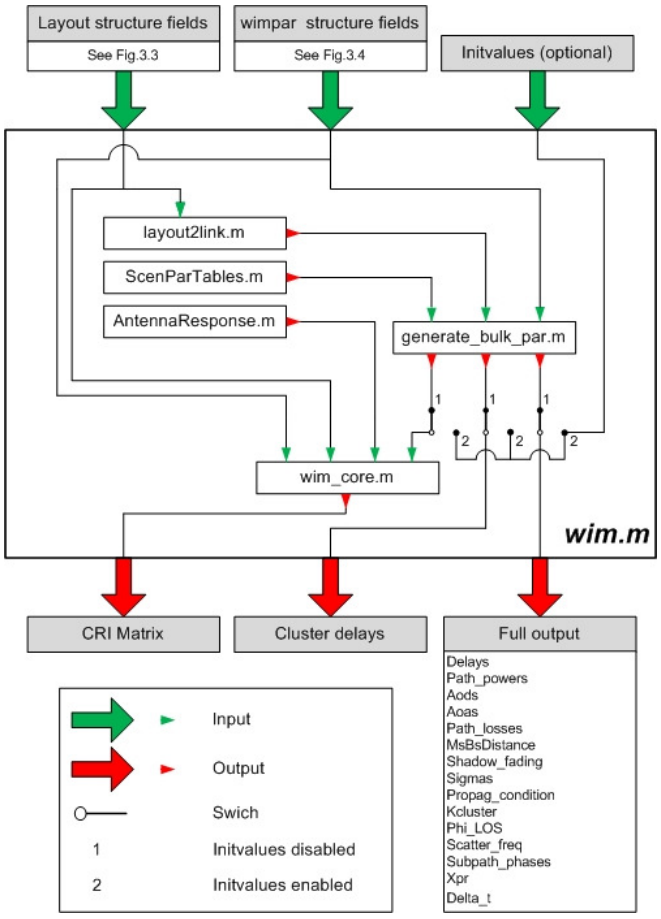

Figure 3.7: wim.m operation diagram

3.2 Code adaptation for Professional Wireless Microphone System, PWMS

The previous section has shown an overview of all the possibilities the WINNER Matlab code provides the user in order to simulate several wireless communication applications including, for each application, the calculation of the channel impulse response. Section 3.2, based in all WINNER Matlab code possibilities, aims to show an adaptation of this code to the needs of the PWMS application under study in this thesis. Firstly the general problem is described, and based on that description, necessary adaptations are explained. As stated along this report, the PWMS application layout must be the same as that described in [Vos08], which chose, as a PWMS application scenario, the Hannover Congress Center (HCC) hall. In those experiments conducted in the HCC hall, the transmission part consisted of one signal generator and one transmitter antenna. The receiver part was formed by one antenna and one vector signal analyzer. Both parts, the transmitter and receiver, were located in the main scenario in where the transmitter was fixed on one position and the receiver stands on the center. The idea was to study the effect of the environment on the signal transmitted using the Saleh-Valenzuela channel model. In this thesis the goal is to compare the impulse response simulations performed by WINNER with the results of [Vos08], adding a study of the channel behavior when the receiver antenna is on movement. This is one of the most important parts here because, while Saleh-Valenzuela model cannot simulate the movement of the terminals, WINNER is able to implement this situation. Thus, the results shown in chapter 4 of this document are focused on comparing the simulations carried out by WINNER model, with the results reported in the [Vos08], as well as to analyze the effect of the movement of the receiver antenna.

This section is structured similarly to section 3.1. The next subsections show the PWMS antennas characteristics and their corresponding code adjustment. Later, the code adaptations for layout parameters and simulation parameters are justified.

3.2.1 Code adaptation for PWMS antennas

The PWMS application radio link network consists of two stations or terminals, one transmitter and one receiver, working in a frequency range of 900MHz and 1.8GHz. The mobile station (MS) antenna typically has horizontal polarization isotropic field pattern, whereas the base station (BS) that acts as a transmitter for this SISO link, exhibits a horizontal polarization whose field pattern is shown in fig.3.8.

(a) (b)

Figure 3.8: (a) 900MHz Schwarzbeck antenna field pattern; (b) 1800MHz Schwarzbeck antenna field pattern

In the WINNER Matlab code, the antenna field patterns are described by a 4-dimensional matrix, so it is necessary to convert the 2D antenna field pattern diagrams shown in fig.3.8, into a 4D matrix in order to be processed by WINNER code. There are three different radiation patterns to create. Two of them correspond to the transmitter antenna. Fig.3.8 shows the different transmitter antenna field patterns (depending on the frequency) that are implemented in this thesis. The third field pattern belongs to the isotropic receiver antenna. Both transmitter and receiver antennas have the same number of elements, 1, and both of them present horizontal polarization. Since both antennas have horizontal polarization, only the azimuth vector is necessary to represent the radiation patterns. For this reason, the size of elevation vector parameter is 1. The last parameters that are required are the number of azimuth samples and the radiation level of each one. The azimuth vector covers 360 degrees from -180^{o} to 179^{o}. The number of azimuth samples depends on the resolution desired. One sample per azimuth degree achieves a good compromise between resolution and computer processing velocity. All these characteristics determine the size of the 4D matrix. The size of the first dimension is 1 because of the number on elements

of each antenna. The size of the second dimension is 2, due to the polarization options, horizontal and vertical. Third and fourth dimension are 1 and 360 respectively, that is, the field pattern samples in elevation are 1 and the field pattern samples in azimuth are 360.

$$FP_{1j} = \begin{pmatrix} 0 & a(1j)_{12} \end{pmatrix} \qquad for 1 \leq j \leq 360 \tag{3.12}$$

In eq.3.12, the first column of the matrix defines the field pattern for vertical polarization. In this case is 0 because the antenna polarization is horizontal. The second column establishes the antenna field pattern for horizontal polarization. In summary, the WINNER field patterns consist of 360 1x2 matrices.

$$\begin{aligned} &(0,a_1) && for \ -180^{\circ} \ of \ azimuth \\ &(0,a_2) && for \ -179^{\circ} \ of \ azimuth \\ &\vdots \\ &(0,a_{360}) && for \ 179^{\circ} \ of \ azimuth \end{aligned} \tag{3.13}$$

Finally, the values for $a_1 ... a_{360}$ have to be set. These values are not decibels but linear values. The isotropic field pattern is built by setting all a values with ones; thereby the field pattern of this antenna is the same for all the azimuth angles.

$$FP_{1j} = \begin{pmatrix} 0 & 1 \end{pmatrix} \qquad for 1 \leq j \leq 360 \tag{3.14}$$

The other two remaining field patterns are constructed from fig 3.8. Taking a few relevant points of these field patterns and interpolating them, Matlab returns a vector with the desired values. Assigning each value calculated by interpolation to each azimuth sample (each coefficient a) in the correct order, the field pattern construction process will be finished. Fig 3.9 shows the construction process steps of the transmitter antenna field pattern at 900MHz. In fig.3.9, the first step represents the original field pattern of the transmitter antenna obtained from the website of the antenna brand, Schwarzbeck, [sch]. In the second step, the most representative points of the shape of the field pattern are marked directly from the original radiation pattern. These points are interpolated, and the values obtained are used to build the 4D matrix that represents the WINNER antenna field

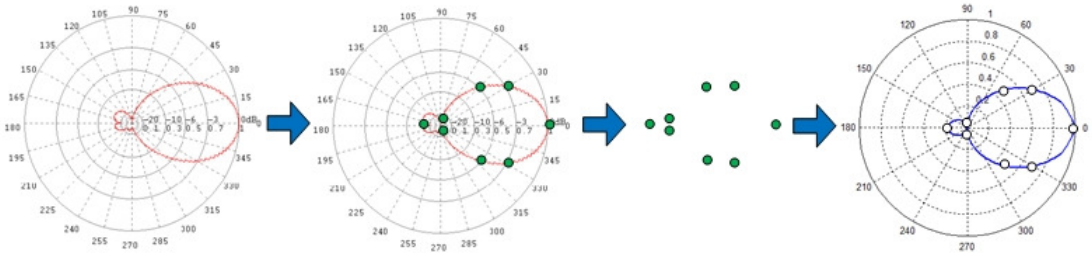

Figure 3.9: Field pattern Matlab implementation process from Schwarzbeck 900MHz antenna model diagram

pattern. This matrix is processed by Matlab creating the radiation pattern that is shown in the last step of fig.3.9.

AntennaArray.m is the WINNER Matlab code file responsible of building up all required antennas for the PWMS application under study. In this case, for each field pattern one antenna is implemented, the isotropic receiver antenna, and the two transmitter antennas, one at 900MHz and the other one at 1.8GHz. Both transmitter antennas never work simultaneously since the PWMS application layout only uses one receiver antenna and one transmitter antenna. Because of each antenna is composed by one element, the input arguments required by *AntennaArray.m* are the azimuth vector and the field pattern, and it is not necessary define the location of the antenna element. As stated in the last section, the three antennas generated are structures that contain the position, rotation and field pattern features. The position and rotation cannot be set in the antenna construction process. The user can adjust them manually, later, at the same time that the simulation layout parameters. Therefore, before this adjustment, the position and rotation are defined by their default values, which are, for both parameters, $[0,0,0]$ [8].

Each antenna structure generated is stored in one Matlab vector; hence, each antenna can be referenced separately. This is relevant to assign each kind of antenna to each kind of terminal (BS or MS). In brief, the field patterns, which are result of the Matlab antenna construction process, are used to simulate the PWMS application. They are presented in the diagrams in fig.3.10.

[8] In Cartesian coordinates.

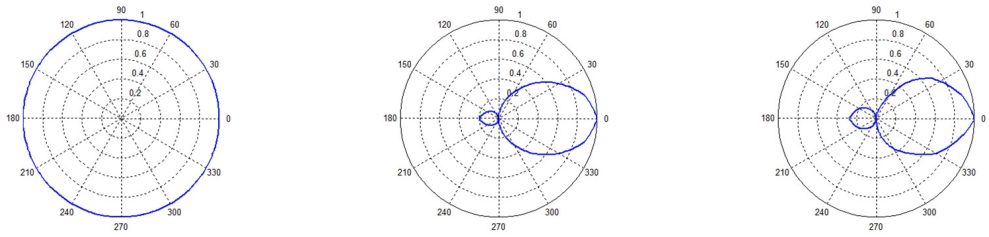

(a) Rx antenna (b) Tx antenna at 900MHz (c) Tx antenna at 1800MHz

Figure 3.10: Field patterns of the antennas used for WINNER simulations.

Figure 3.11 summarizes the parameters that need to be modified to build up the PWMS application layout using WINNER Matlab code. It also includes the appropiate value for each parameter.

AntennaArray.m	
INPUTS	OUTPUTS
Field Pattern = Schwarzbeck or isotropic field pattern **Azimuth vector** = 360 elements from -180 to 179 degrees **Num of elements** = 1	

Figure 3.11: Matlab parameters of the PWMS antennas

3.2.2 Code adaptation for PWMS network layout parameters

The layout parameters are set using the file *layoutparset.m*. Some of them are set before executing this file, as inputs, and the others doing modifications in the *layoutparset.m* output structure. The inputs used are:

- Number of links.
- The maximum radius of the simulated area.
- The Matlab vector composed of the antenna structures.
- The characteristics of the terminals used in the PWMS application.

As seen in fig.3.4, the output of *layout parset.m* is a structure containing the layout parameters that WINNER code offers. Not all these parameters are relevant, so some of them conserve their default values or are disabled. To understand the code modifications that take place in this section, fig 3.12 shows the basic layout diagram in where [Vos08] obtained the channel impulse response data, and that is the same as used in this thesis to simulate the PWMS application.

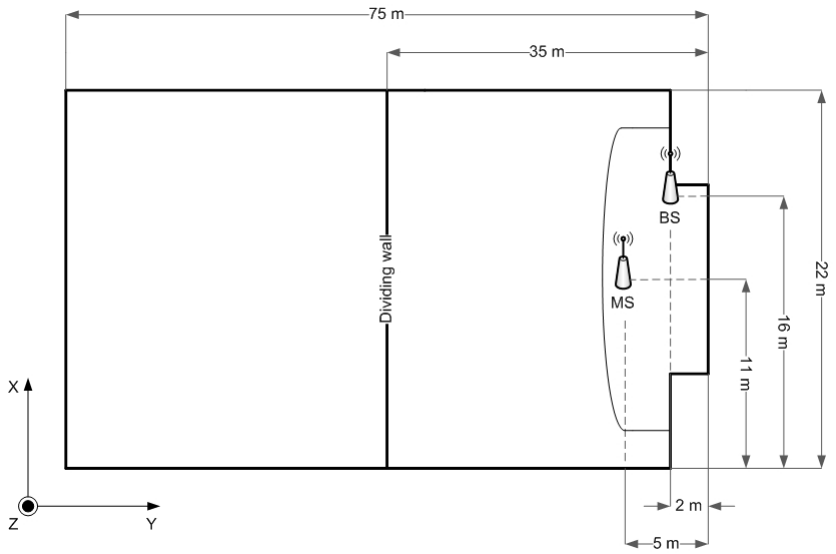

Figure 3.12: HHC hall basic scheme

The PWMS application is formed by one MS and one BS, so there is one link in this radio communication system, the link between the base station and the mobile station. The base station (the transmitter) has one sector and depending on the work frequency, its antenna is one of the two Schwarzbeck models, 900MHz or 1.8GHz. The mobile station (the receiver) is formed by an isotropic antenna. From these characteristics, the inputs of the function *layout parset.m* for this application are set up as follows:

- Antenna arrays. This is a Matlab matrix that contains the different antenna structures generated before by *AntennaArray.m*. In this case, the 900MHz antenna is the first element of the vector, the 1.8MHz antenna is the second, and the isotropic antenna is the third.

- Mobile stations. This 1x1 Matlab matrix whose value is equal to the ”Antenna arrays” vector index which points to the isotropic antenna. 2. Since the isotropic antenna is the third element of Antenna arrays, the value of Mobile stations is 3.
- Base stations. Since both base stations (one for 900MHz and the other one for 1.8GHz) have only one sector, this parameter is a 2x1 Matlab matrix [9] in which the first element is equal to the ”Antenna arrays” vector index which points to the 900MHz antenna, 1, and the second element is equal to the ”Antenna arrays” vector index which points to the 1.8GHz antenna, 2.
- Maximum radius of the simulated area. The longest side of the Hannover Congress Center hall determines the value of this parameter. In this case, 71 meters.
- Number of links. There is only one link, the link between BS and MS, so this parameter is equal to 1.

Some PWMS application layout features are set in the input arguments of *layout parset .m*, but there are others that have not been specified yet. Like stated in subsection 3.1.2, the *layout parset .m* output is a structure that contains the layout information that *wim.m* needs to calculate the CIR matrix. The remaining features are introduced by changing some parameters of this output structure. In order to perform the CIR simulations under an environment as close as possible to [Vos08] environment, the first step is to choose the best scenario, of all that the WINNER model provides, that fits better to the PWMS application analyzed in [Vos08]. However, the experiments conducted in that report were performed with no people inside simulated area but all the WINNER scenarios assume mobile elements in the environments like people or traffic. This problem cannot be solved due to limitations in the WINNER Matlab code, therefore, this difference in the simulated environment must be taken into account when comparing the Saleh-Valenzuela channel model and the WINNER channel model. Ignoring this issue, the suitable scenario for this application is the B3. The WINNER B3 scenario describes the typical indoor big hall where high density of people and furniture is expected. This is exactly the type of environment of the HCC hall, one big room with lot of tables, chairs and columns, prepared to accom-

[9] In case that the base stations presented more than one sector, this parameter would be a Matlab Cell Array.

modate many people for big ceremonies, conferences or even concerts. The WINNER scenario is set by modifying the parameter *ScenarioVector*.

Another output field that is necessary to modify is *Stations*. *Stations* is a structure that shows the MS and BS information in terms of position, rotation, antenna features and station velocity. At this point, the antenna field patterns are already calculated, so in this process only it is necessary to modify the location and velocity of the stations. $Nofsect$ is only an information parameter that defines the number of sectors of the terminals. *Pairing* establishes the links between the terminals. In this case this parameter has a fixed value because there is only one link in this PWMS application. $NumFloors$, $NumPenetratedFloors$, $Dist1$, $StreetWidth$ are not important for this PWMS application. The relevant layout parameters and its modifications are listed below.

- *ScenarioVector.* The file *ScenarioMapping.m* assigns one index to each scenario. In this case the index of B3 scenario corresponds with the number 5, and as there is only one link (K=1), the value of *ScenarioVector* is 5.
- *PropagConditionVector.* WINNER cannot simulate LOS and NLOS condition for one link at the same time. Hence, this parameter is set to 1 or 0 depending on the propagation condition to match the simulation of the PWMS application.
- *StationPosition*. This parameter is a 1x3 Matlab matrix that contains the station position in cartesian coordinates, $[x,y,z]$. From fig.3.12 the x and y coordinates of BS and MS are $[16,2,z]$ and $[11,5,z]$ respectively. The z coordinate represents the height in where the antenna of each station is located. In the [Vos08] measurements, the transmitting antenna was mounted on a mast about 2 meters in height, while the receiving antenna was fixed to the belt of a test person about 1.80 meters tall, that is at a height of 1 meter approximately. From this, the initial position in cartesian coordinates of each station is $[16,2,2]$ for BS and $[11,5,1]$ for MS. The position of BS is fixed but it is necessary to change the MS position after the first simulation in order to simulate the mobile station movement. Simulations must be run for several different MS positions. These changes are shown and described in the next chapter.
- *StationVelocity*. For BS, the station velocity cartesian components can be set as [0,0,0] meters per second because the base station is fixed during simulation process.

For MS, for simulating the movement of the antenna, the velocity of the MS is the average speed of a person, 5 km/h. 5 km/h is equivalent to 1.39 meters per second or, in WINNER format $[\pm 0.8, \pm 0.8, \pm 0.8]$ m/s. The choice of $+$ or $-$ determines the direction of MS. One WINNER Matlab code limitation is that the MS velocity cannot be set to 0 m/s because the Ms velocity is a term that belongs to the denominator of eq.3.7 which calculates the simulation time sample interval. This can be a problem when comparing the WINNER model with [Vos08] results since these results are based on measurements in which the stations were fixed. To avoid the effect of movement, and thus, be able to compare the results, the MS velocity is adjusted to a value low enough to assume that the terminal is not moving. In this case the MS velocity is set to $1e^{-5} m/s$.

- *StationsRotation*. $[Rot_x, Rot_y, Rot_z]$ is the antenna rotation by respective axes of GCS. This means that Rot_z determines the azimuth angle whereas that Rot_y sets the elevation angle. The rotation of the MS is not necessary because its field pattern is omnidirectional in terms of azimuth. Only azimuth rotation of BS will be performed in this thesis using the next equation and taking into account the fig.3.13.

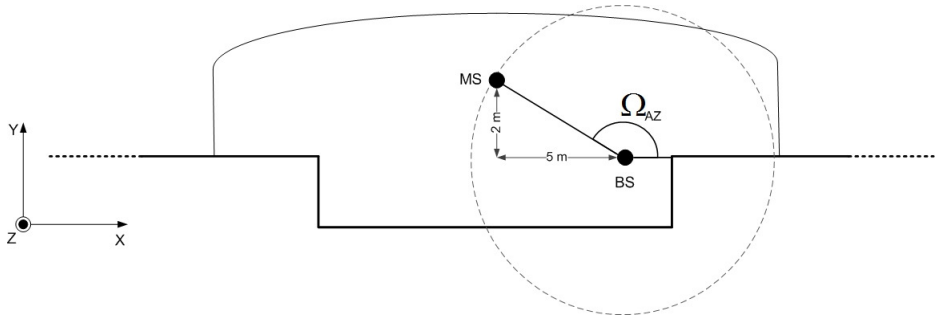

Figure 3.13: Azimuth angle between stations

$$\begin{aligned} \Omega_{AZ}(rad) &= \pi - arctan(\frac{Y_{MS} - Y_{BS}}{X_{BS} - X_{MS}}) \\ \Omega_{AZ}(rad) &= 3.1416 - arctan(\frac{5-2}{16-11}) = 2.6011 rad \approx 150^{\circ}. \end{aligned} \tag{3.15}$$

A summary of modifications in the layout parameters described in this section is shown in fig.3.14.

layoutparset.m	
INPUTS	OUTPUTS
Mobile Stations = 1 **Base Stations** = 1 **Number of links** = 1 **Maximum radius** = 71 m	**ScenarioVector** = 5 **PropagConditionVector** = 1 (LOS) or 0 (NLOS) **MS position** = [11, 5, 1] m **MS velocity** = [0.8, 0.8, 0.8] m/s or [5.77e-6, 5.77e-6, 5.77e-6] m/s **BS position** = [16, 2, 2] m **BS rotation** = [0, 0, 2.6011] rad

Figure 3.14: Summary of modifications in the relevant *layoutparset.m* parameters

3.2.3 Code adaptation for PWMS general simulation parameters

In this subsection, the general WINNER simulation parameters are set in order to obtain PWMS simulations which can be compared with [Vos08] results. As it happened before with the antenna and layout parameters, not all the general simulation parameters described in subsection 3.1.3 are extended in this subsection.

This thesis aims to simulate the channel impulse response of the PWMS application using the WINNER features for a B3 scenario. The calculation of pathloss is not a priority, therefore, the parameters *PathLossModel*, *PathLossOption*, *PathLossModelUsed*, *ShadowingModelUsed*, which are related with the function *pathloss.m*, are not necessary to change and study. On the other hand *Range* and *end_time* can be neglected because these parameters are only implemented for one specific WINNER scenario different than the B3. Due to the PWMS layout structure in which only one link is simulated, *UniformTimeSampling* parameter is irrelevant. *PolarisedArrays* is also an unnecessary parameter because although it is enabled, actually its influence in the simulation is zero since both the transmitter and receiver antenna have only horizontal polarization.

There are general simulations parameters that will not have a fixed value. This is the case of *FixedPdpUsed FixedAnglesUsed*. These parameters have two possible states, 'yes' (enabled) or 'no' (disabled). If both parameters are enabled the cluster power, cluster delay and angle parameters are fixed values determined by the CDL model explained in subsection 3.1.3. If, on the contrary, both parameters are disabled, the cluster power, cluster delay and angle parameters are generated randomly. The random generation of these parameters may mask some effects, precluding the measurement and analysis of them. For example, to test the effect the MS movement in the CIR matrix, it is necessary run

some simulations. The expected changes between different simulations are small so these changes could be confused with the random variations of the cluster features. In this case the value of *FixedPdpUsed* and *FixedAnglesUsed* must be 'yes'. However, for statistical analysis of the CIR matrix, the randomness of the cluster features is necessary because otherwise, in all simulations, the CIR's obtained would be practically the same and the conclusions about results could be unreliable. In this case, the value of *FixedPdpUsed* and *FixedAnglesUsed* must be 'no'.

With regard to other simulation parameters, there are some of them in which it is not necessary to change their default values and there are others whose value determines different setups in the simulation process like, for example, the simulation duration or propagation condition. All these parameters are listed below:

- *NumSubPathsPerPath*. The default value of this parameter is 20 and it follows the WINNER basic theory concepts explained in chapter 2.
- *DelaySamplingInterval*. This parameter is set to $5e^{-9}$ seconds.
- *RandomSeed*. There is no seed for WINNER random generators, so its value is an empty Matlab vector.
- *TimeEvolution*. There is no option to change this value; it is always set to 'no'.
- *CenterFrequency* (f_c). Like stated in last section, the WINNER channel model just depends on the *CenterFrequency* in the case of path losses estimations and also in the time sample interval (ΔT) calculation (see eq.3.7). This means that, for CIR computations, the *CenterFrequency* is an irrelevant parameter except for determining the time sample interval. High values of time sample interval cause significant changes in the channel impulse response, from one time sample to other. In this case, cluster time evolution is highly variable, whereas small values of ΔT make the CIR matrix nearly constant in time. The *CenterFrequency* is set to $9e^8$ (900MHz) or $1.8e^9$ (1.8GHz) depending on the antenna in use. Returning to eq.3.7 and since both the velocity of the MS and *CenterFrequency* are established, the parameter that determines the ΔT is *SampleDensity*.
- *SampleDensity* (*Sd*). First of all, for successful a Doppler analysis, *SampleDensity* should be more than 1. If the values of MS velocity, number of time samples and

CenterFrequency are set, high values of *SampleDensity* decrease the value of the time sample interval (see eq.3.7). On the contrary, small values of *SampleDensity* increase the value of the time sample interval. The higher the value of this parameter, the lower the variation of each cluster along the time. Fig.3.15 shows the time evolution of the three strongest clusters in a B3 scenario, depending on the SampleDensity value when the MS velocity, number of time samples and *CenterFrequency* are fixed. For example, in the case that f_c is 900MHz and MS velocity is 10 meters

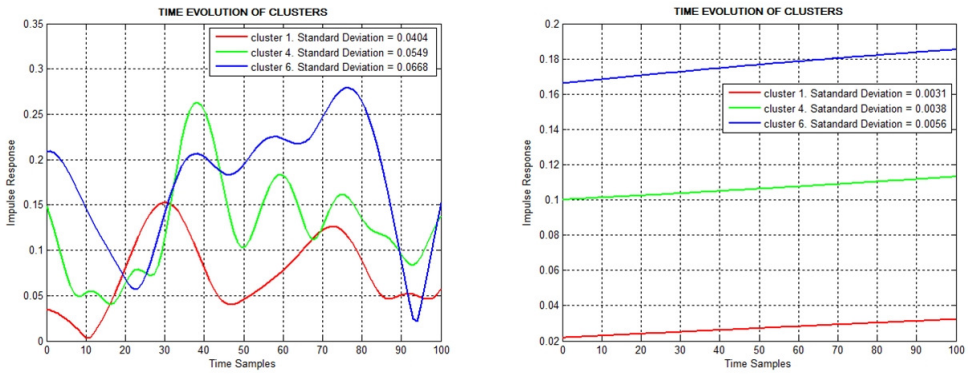

(a) SampleDensity=2 (b) SampleDensity=100

Figure 3.15: Time cluster evolution depending on the SampleDensity

per second the time sample interval is:

$$\Delta T = \frac{\lambda}{2(v_{MS} \times sd)} = \frac{\frac{c}{f_c}}{2(v_{MS} \times sd)} = \frac{\frac{3 \cdot 10^8 m/s}{0.9 \cdot 10^9 Hz}}{2(10m/s \times 2)} = 0.0083s. \tag{3.16}$$

Knowing that $\lambda = 0.33m$, and for $SampleDensity = 2$ there are 2 time samples per half wavelength, that is, WINNER takes 2 time samples per $0.165m$. If the number of time samples is set to 100, WINNER finishes the simulation in $0.83s$ and take 100 time samples per $8.25m$. For $SampleDensity = 100$ there are 100 time samples per half wavelength, that is, WINNER takes 100 time samples per $0.165m$ which is the total number of samples. Comparing both results, in the first case there is more information about the cluster time evolution, as it shown in fig.3.15 a). When the value of *SampleDensity* is set to 100, WINNER take all the samples in a short

space so there is very little information about cluster time evolution and as, fig.3.15 b) shows, the clusters seem time invariant for $0.83s$ of simulation.

- *IntraClusterDsUsed*. As discussed repeatedly throughout this thesis, one of the main objectives is to compare the WINNER CIR calculated in chapter 4 with the Saleh-Valenzuela CIR implemented in [Vos08] Fig 2.5 shows the typical shape of Saleh-Valenzuela channel impulse response in which the rays are grouped forming a cluster, and in where it is possible to see the cluster delay dispersion. Generally, the cluster delay spread in the WINNER channel model is zero. However, setting *IntraClusterDsUsed* to 'yes', WINNER permits to see the delay dispersion of the two strongest clusters. To facilitate the comparisons between the two models, the *IntraClusterDsUsed* parameter is set to 'yes'.

- *UseManualPropCondition*. This parameter is set to 'yes' because in this way, WINNER allows the user to change the propagation condition (LOS or NLOS) manually as required.

- *NumTimeSamples*. High values of this parameter provide more time information of the channel impulse response but, also, need more processing time. This value is set in the next chapter, depending on the number of time samples used in [Vos08] experiments.

A summary of modifications in the simulation parameters described in this section is shown in fig.3.16.

wimparset.m	
INPUTS	OUTPUTS
	FixedPdpUsed = 'yes' or 'no' **FixedAnglesUsed** = 'yes' or 'no' **CenterFrequency** = 900 MHz or 1800MHz **SampleDensity** = 2 (time evolution) or 100 (stationary channel) **IntraClusterDsUsed** = 'yes' **UserManualPropCondition** = 'yes' **NumTimeSamples** = 100

Figure 3.16: Summary of modifications in the relevant *wimparset.m* parameters

4 PWMS scenario

So far, chapter 2 has reported the main problem discussed in this thesis and has explained the basic theoretical concepts needed to understand it. In the chapter 3, the tools necessary to achieve the WINNER CIR computer simulation have been described. The second part of this third chapter shows how to use these tools in order to compare the WINNER channel model simulations obtained with the Saleh-Valenzuela channel model simulations carried out by [Vos08]. Chapter 4 begins with a detailed description of the HCC hall, which is the scenario used to calculate the WINNER and Saleh-Valenzuela channel impulse response. This description covers the physical environment as well as the expected behavior of the transmitted signal inside the application scenario, that is, how the hall structure can affect the communication between the transmitter and the receiver antenna. It is essential to understand the possible fading effects inside the HCC hall and why they are originated in order to evaluate correctly the results of [Vos08]. Additionally, this chapter makes a study of how different WINNER Matlab code parameters can affect the WINNER simulations, including the movement of the mobile station. Finally, the equivalence between both channel models is discussed. Prior to this, it is necessary to adjust and modify the output CIR format of each model as far as possible to achieve comparability among them. The mechanisms used for this purpose also are explained.

4.1 Hanover Congress Center, HCC

This section aims to describe in detail the scenario in which the channel impulse response measurements were conducted by [Vos08]. From this data collected, and using a modelling process based on Saleh-Valenzuela channel model, [Vos08] calculated the channel impulse response of the HCC hall. The measurement process and the conditions in which

it was performed are also described. As mentioned in section 2.4, the WINNER channel model allows getting the channel impulse response for different scenarios. One of them, called B3, is the most similar to the HCC hall, but not the same. Therefore, it is necessary, within the possibilities offered by the WINNER Matlab code, to set the WINNER layout parameters so that the simulation scenario fits the HCC hall structure as much as possible.

The modelling process is conducted entirely on a computer. This means that the WINNER simulation scenario is not a real place but is a description made by the user. Like stated in chapter 2 and 3, the different WINNER scenarios characteristics are defined based on the measurement campaigns made by [Kyöb]. The user can only choose the WINNER scenario type (from A1 to D2), the simulation area and the position of the transmitter and receiver antennas. This limitation causes the first problem when comparing both models: while [Vos08] calculates the CIR of the HCC hall, in this thesis the CIR calculations are performed on a virtual scenario, which should be as close as possible to HCC hall. In the next subsections, the real and virtual HCC halls are described as well as the expected behavior of the transmitted signal inside these scenarios.

4.1.1 Real HCC hall

Fig.4.1 shows the map of the HCC hall used for channel impulse response measurements (for more information see [HCC]). The transmitter and receiver antennas, BS and MS respectively, are located on stage. There are two lines of columns along the hall, parallel to the sidewalls. In fig.4.1, the columns, represented by (a), are the small rectangles that are on both sides of the hall. Also, there is a dividing wall, (b), in the middle of the hall that divides it into two parts. The back wall is represented by the letter (c).

Like stated in section 2.1, the radio links present multipath propagation caused by reflection, diffraction and scattering. These degrading effects are related to the wavelength of the transmitted signal and the electric size of the objects that obstruct the signal along its path. In the [Vos08] experiments performed in the HCC hall, the center frequency of transmission was 740MHz. This feature determines, using eq.2.2, the value of the signal wavelength, 0.4 meters. From this value, obstacles with a smooth surface whose size are

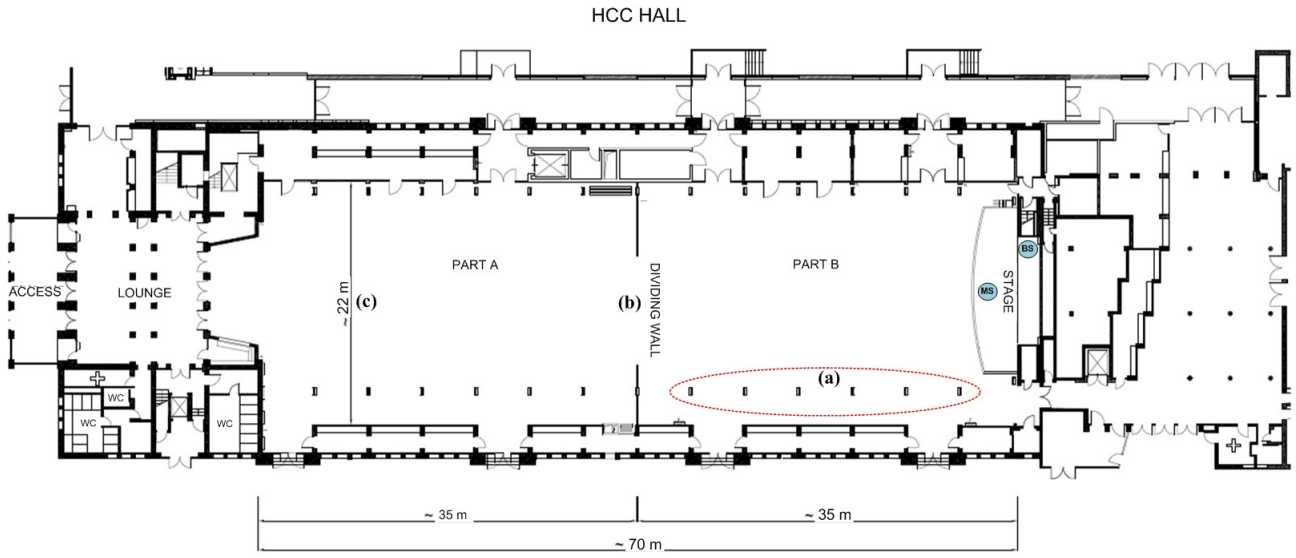

Figure 4.1: HCC hall map.

greater than 0.4 meters, act like reflecting objects. Big dense objects also produce fading effects on the transmitted signal like diffraction. Rough surfaces or small objects may be the cause of signal scattering. When the [Vos08] measurements were taken, the hall was empty of people and furniture so reflection and diffraction effects are, mostly, the cause of the signal multipath propagation. In other words, the walls, the roof, the columns along the hall, the floor and the dividing wall are the main obstructing factors that cause the multipath propagation in this PWMS application.

As seen along the chapter 2, in the Saleh-Valenzuela channel model, the multipath propagation paths are called rays and arrive to the receiver in groups called clusters. As reported in [Mol] [Kyöa] [Zha], the WINNER channel model clusters are constituted by a fixed number of rays, or propagation paths, diffused in angle domains. The rays within the same cluster have the same propagation delay, and the power dispersion of a cluster in angle domains is characterized by cluster angular spread of departure (ASD) and cluster angular spread of arrival (ASA). However, the Saleh-Valenzuela channel model is based on the concept that the rays, which form the clusters, reach the receiver in different

moments due to the path length. As reported in [Sal], the clusters are formed due to the effect of the building superstructure on the transmitted signal, while the individual rays are formed because of the objects that are near to the transmitter and receiver. Inside the HCC hall, the divided wall and the back wall may be the superstructure that form the clusters, whereas that, the corners, windows, door and window frames, columns, etc, are the fading agents responsible for the formation of the different rays within each cluster.

Fig.4.2 shows a schematic of how the clusters would create. In Fig.4.2 a) the direct ray from BS to MS is the first ray that reaches the receiver antenna, that is, the first ray of the first cluster. Successive rays arrive at MS with a time delay. These rays are weaker in terms of energy due to the rebounds with the scatter agents and because their path between, BS and MS, is longer. The numbers in each ray represent the ray arrival time. The number one is the first to reach the receiver because its path is the smallest and so on. The time delay of each ray is represented by τ, as it is shown at the right side of each graph (a, b and c), and gives an example of the formation of an impulse response, cluster by cluster. In Fig.4.2 b), from all the rays that are reflected in the dividing wall, the main ray is the one first that reaches the receiver. Successive reflected rays from the dividing wall arrive at MS later and with less energy forming, thus, the second cluster. Not all the rays that reach the dividing wall are reflected to the MS. Some of them cross through it, due to the diffraction phenomenon, reaching the back wall in which they are reflected, returning to the dividing wall. At this point, some rays are reflected again to the back wall and others are diffracted reaching the MS. Fig.4.2 c) shows these group of rays that, leaving from the BS, are not reflected in the dividing wall but go through it two times before reaching the receiver, one from the transmitter and the other one from the reflection with the back wall. These rays form the third cluster. The energy of the rays belonging to the third cluster is very small compared with the first and second cluster rays. Indeed, the last rays of the third cluster are practically unpredictable, so that no more cluster arrivals are expected. In summary, the expected channel impulse response of this PWMS application inside the real HCC hall is formed by three clusters: the first one due to the direct ray between transmitter and receiver, the next one because of the reflection of rays in the dividing wall, and the last one due to the reflection in the back wall, of the rays that had been previously diffracted in the dividing wall.

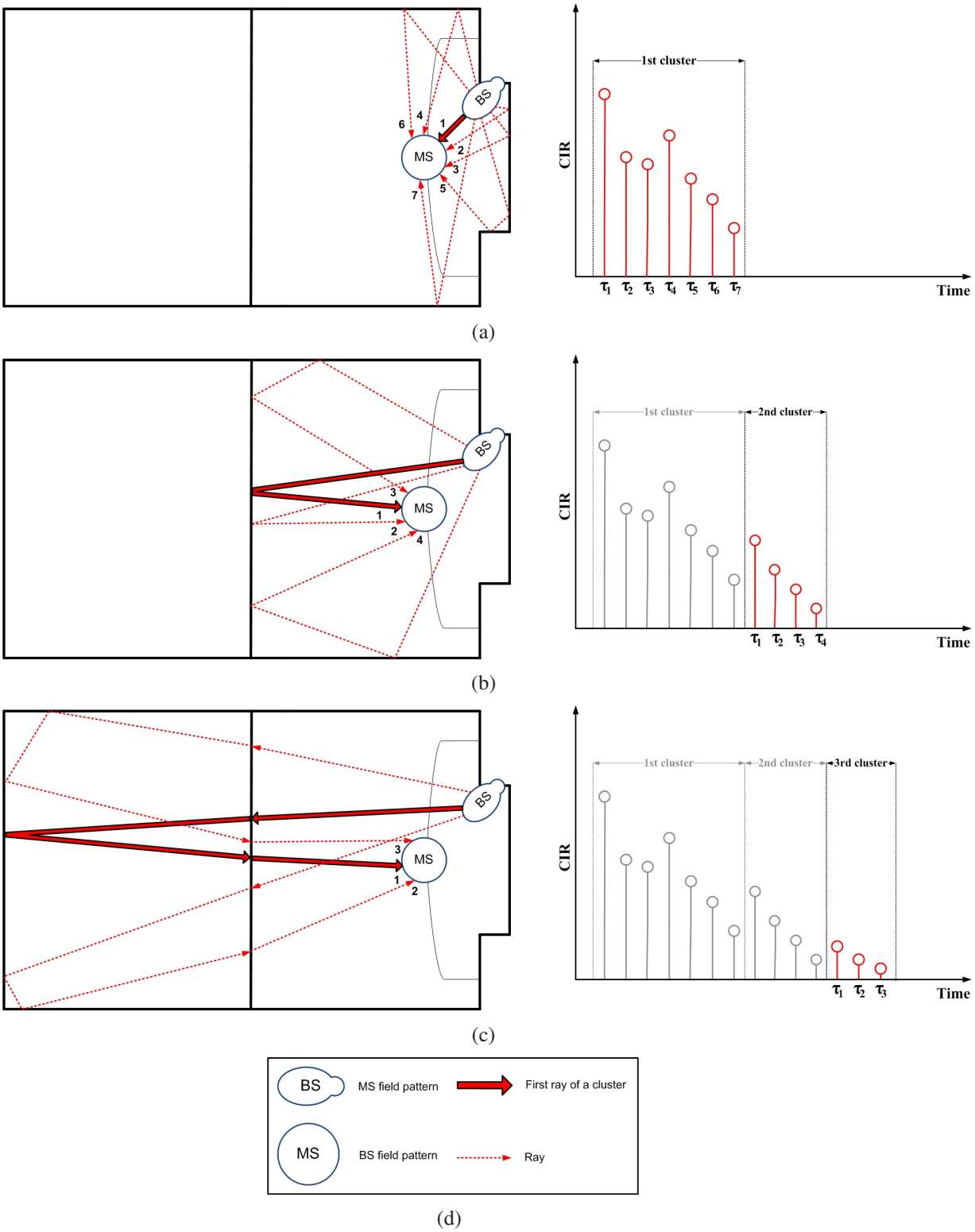

Figure 4.2: (a) Generation of the first cluster; (b) Generation of the second cluster; (c) Generation of the third cluster; (d) Legend

4.1.2 WINNER virtual HCC hall

The virtual HCC hall is the application scenario built from the modifications in the WINNER layout parameters, taking into account the characteristics of the real HCC hall structure.

The WINNER channel model only allows the user to define the scenario type (from A1 to D2), the position of the antennas in GCS and the maximum radius of the simulation area. However, the limitations are even greater because the last two configuration options, the maximum radius and the antenna positions in GCS, are mutually exclusive. Unlike the real scenario in where the stations are inside the simulation area, in the virtual HCC defined by the WINNER Matlab code, the stations delimit the simulation area, that is, they are the boundaries. When the user defines the maximum radius of the simulation area, the WINNER code randomly calculates the position of the antennas taking into account that the distance between the respective x and y coordinates of both antennas never exceeds the radius selected. Thus, the transmitting and receiving antennas have always different locations for each WINNER simulation. By contrats, if the positions of the antennas are fixed to a certain place, the maximum radius of the simulation area becomes irrelevant. Therefore, there are two possible options, shown in fig.4.3, for simulate the HCC hall:

1. Keep the positions of the antennas described in [Vos08] in exchange for a considerable reduction of the simulation area.
2. Set a simulation area of similar size to that of the real scenario, but considerably increasing the distance between both antennas.

Both configurations are not quite good solutions, so it is necessary to take in mind this WINNER code limitation when analyzing the WINNER simulations. After simulate two simple WINNER examples using these configurations, it is observe that the amplitude of the last [10] clusters are practically the same for both cases, while the first clusters suffer a reduction in amplitude of nearly $3dB$ when using the second configuration option. This feature is due to the distance increase between the BS and MS. Since the first configuration sets the same distance between the transmitter and the receiver as in the real scenario, and

[10] In time domain.

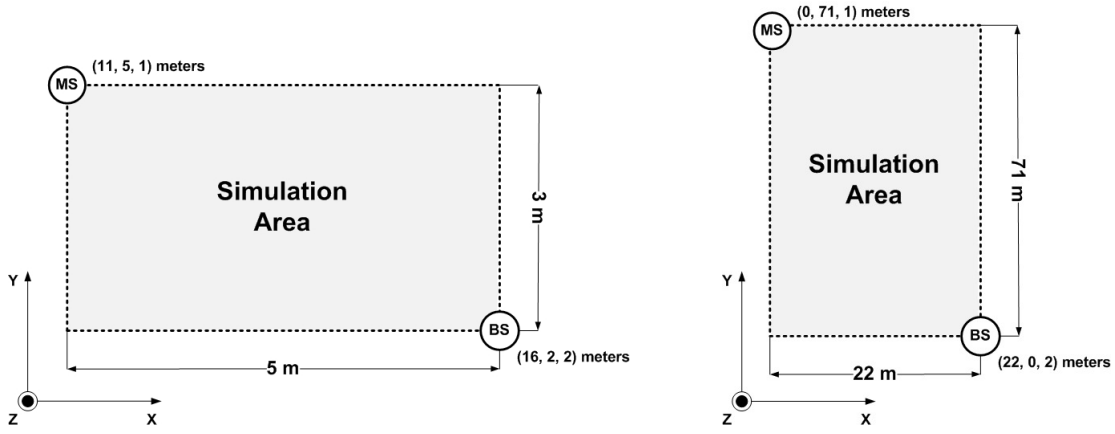

Figure 4.3: WINNER layout configuration options

since, both options present very similar amplitudes for the last clusters, the ”least bad” configuration is the first one, corresponding to the fig.4.3 a).

Actually, last layout features are not the key layout configuration options that make the WINNER model fits well a certain environment, in this case, the HCC hall. As a statistical channel model, the WINNER model do not take in mind the physical characteristics of any scenario but it is based in measurement campaigns carried out in several environments in order to cover, as far as possible, all wireless communications scenarios. For this reason the most important layout configuration option that the WINNER Matlab code provides is the scenario type. This parameter largely determines the WINNER channel impulse response.

The WINNER scenario that fits better the characteristics of the HCC hall is the B3 hotspot scenario. The basic features that make the B3 scenario the most suitable of all WINNER scenarios for this PWMS application are:

- Built up for large indoor halls, like train stations, airports or conference halls.
- The typical dimensions of this scenario are between 20x20 meters to 100x100 meters in length and width, and up to 20 meters in height

- The Velocity of the stations is between 0 and 5 km/h [11].
- B3 scenario is defined for LOS and NLOS case. In the simulation scenario using in [Vos08] there was no objects obstructing the path between the transmitter and the receiver. However, as explained below in subsection 4.3.1, the simulations in the WINNER B3 scenario for this PWMS application are run in LOS and NLOS cases.

The WINNER B3 scenario, for LOS case, is formed by 10 clusters with 20 rays per each cluster. However, if the parameter $IntraClusterDsUsed$ is enabled, the number of clusters increased to 14 [12], due to the division of the two strongest clusters into three subclusters in order to simulate the cluster delay dispersion. For all the WINNER scenarios, there are two type channel models, the generic model and de cluster delay line model. As discussed in subsection 3.2.3, the use of each model will depends on the type of simulation required. Accordingly, the time arrival, power, AoA and AoD of each clusters will depend on the type of B3 scenario channel model used.

Generic model. In the generic B3 model the cluster delays and power are generated following an exponential distribution and based on several parameters which are shown in table 4.1. This table has been built from the parameters described in [Kyöb]. The time de-

Parameters	B3 Scenario. LOS case
Delay spread ($log_{10}([seconds])$)	mean(μ) = -7.44; standard deviation(σ) = 0.12
K-Factor(K)[dB]	mean(μ) = 2; standard deviation(σ) = 3
Delay distribution	Exponential
Number of clusters	10 or 14 ($IntraClusterDsUsed = enabled$)
Number of rays per cluster	20
Per cluster shadowing std ζ	3

Table 4.1: B3 LOS generic model parameters involved in the calculation of cluster delays and cluster powers

lay of the nth cluster for the WINNER B3 scenario is calculated using the next expression

[11] In the PWMS scenario under study, it is assumed the possibility of quick turns of the MS, and people walking and blocking the communication between BS and MS.

[12] For NLOS case there are 15 clusters composed by 20 rays per each cluster. In the same way as LOS case, if $IntraClusterDsUsed$ is enabled, the number of clusters is increased to 19.

previously defined in [Kyöb]:

$$\tau_n = -r_\tau \sigma_\tau ln(X_n), \tag{4.1}$$

where r_n is the delay distribution proportionality factor, σ_τ is the delay spread and X_n is an uniform distribution from 0 to 1, $U(0,1)$. For LOS case it is required to calculate a scaling constant, D, which depends on the Ricean K-Factor in this way

$$D = 0.7705 - 0.0433K + 0.0002K^2 + 0.000017K^3. \tag{4.2}$$

Finally, the time delay of the WINNER B3 scenario for LOS case is

$$\tau_n = \tau_n / D. \tag{4.3}$$

The cluster powers are calculated as shown in the following equation

$$P_n = exp\left(-\tau_n \frac{r_\tau - 1}{r_\tau \sigma_\tau}\right) \cdot 10^{\frac{-Z_n}{10}}, \tag{4.4}$$

where Z_n is the per cluster shadowing term in dB following a normal distribution between 0 and ζ. $Z_n = N(0,\zeta)$. If M is the number of rays per cluster, the power of each ray within nth cluster will be P_n/M. [13] In summary, each WINNER B3 generic model simulation generates a channel impulse response in which the cluster parameters are based on table 4.1 and equations 4.1 to 4.4, that is, each simulation is a random channel impulse response realization. As stated in subsection 3.1.3, a set of these realizations gives the typical B3 cluster features values which are picked up in the CDL tables that make up the CDL model.

CDL model. In the cluster delay models, the cluster delay, power and angle characteristics are fixed to typical values to obtain comparable simulation results. Moreover, in case of $IntraClusterDsUsed$ is enabled, the CDL model for the WINNER B3 scenario determines that the two strongest clusters are in general the second and sixth. The cluster parameters of this scenario [14], when the CDL model is used, are presented in tables 4.2 and 4.3 which were previously shown in [Kyöb].

[13] Equations 4.2, 4.3 and 4.4 comes from [Kyöb].
[14] For LOS propagation case.

Cluster number	Delay (ns)	Power (dB)	AoD (º)	AoA (º)
1	0	0	0	0
2	0	-9.6	-23	-53
3	15	-14.5	-34	-79
4	25	-12.8	-32	-74
5	40	-13.7	33	76
6	40	-14.1	-35	80
7	90	-12.6	32	-73
8	130	-15.2	-35	80
9	185	-23.3	-43	-100
10	280	-27.7	47	-108

Table 4.2: WINNER B3 scenario CDL model parameters when *IntraClusterDsUsed* is disabled. LOS case

Cluster number	Delay (ns)	Power (dB)	AoD (º)	AoA (º)
1	0	0	0	0
2	0	-9.6	-23	-53
3	5	-11.8	-23	-53
4	10	-13.6	-23	-53
5	15	-14.5	-34	-79
6	25	-12.8	-32	-74
7	40	-13.7	33	76
8	40	-14.1	-35	80
9	45	-16.4	-35	80
10	50	-18.1	-35	80
11	90	-12.6	32	-73
12	130	-15.2	-35	80
13	185	-23.3	-43	-100
14	280	-27.7	47	-108

Table 4.3: WINNER B3 scenario CDL model parameters when *IntraClusterDsUsed* is enabled. LOS case

In addition, the CDL values of the cluster ASD and ASA are 5º and 5º respectively. [15] The grey rows of table 4.3 represents the subclusters, which simulates the cluster delay spread of the second and sixth cluster of table 4.2.

[15] Always in the case of WINNER B3 scenario.

Fig.4.4 shows the power delay profile, PDP, of a WINNER B3 scenario simulation when the CDL values presented in table 4.2 are used. For this simulation, the layout scheme is the same as that presented in fig.4.3 (a). [16]

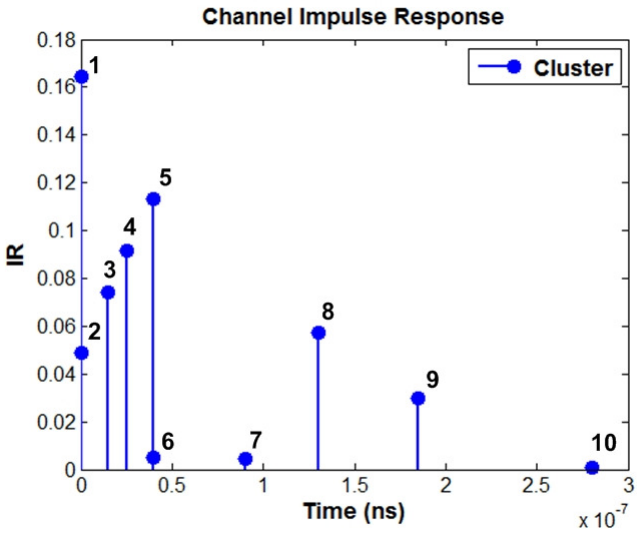

Figure 4.4: WINNER B3 scenario PDP of CDL model. LOS propagation case.

From fig.4.4, the first cluster is due to the multipath components that reach the receiver, first. The 2nd, 3th and 4th, probably are formed because of the signal reflection and diffraction on scatters that are placed near to the receiver. The clusters number 5, 8 and 9 seems to be caused by room walls or big scatters such as people or elements of the building structure located not so far. Last cluster usually is the result of the signal reflection on the back walls, roof corners, etc, placed in the other side of the indoor environment, away from the receiver. The time delay of each cluster correspond to the values of the second column of table 4.2. In all WINNER B3 scenario simulations that use the CDL tables, each cluster has always the same delay time. The amplitude of each cluster depends on the layout setup, the cluster angle parameters and cluster power from tables 4.2 and 4.3. Unlike the delay values, the amplitude levels for the same cluster are not equal although the simulations are carried out under the same conditions. The amplitude variations for each CDL simulation are given by changes in the simulation scenario layout (stations po-

[16] The cluster amplitude values correspond with the mean of the cluster amplitude time evolution (see fig.2.4).

sition and rotation) and the randomness of large scale parameters such as Ricean k-factor, shadow fading and the angle features of the rays within the clusters. This randomness is uncontrollable and may hide, in the CIR graphs, the consequences of small changes in the scenario layout, that is, in some cases it could be impossible to predict whether the changes in amplitude are produced by the large scale parameters variations or by changes in the simulation setup. The table 4.4 shows an example of these variations when 10 different simulations are performed under the same layout conditions that the used to simulate the PDP of fig.4.4.

Cluster number	Sim1	Sim2	Sim3	Sim4	Sim5	Sim6	Sim7	Sim8	Sim9	Sim10	Mean
C1	0.0318	0.0281	0.0488	0.0290	0.0084	0.0320	0.0439	0.0851	0.0721	0.0298	0.0409
C2	0.1874	0.1298	0.0884	0.3223	0.0259	0.1815	0.2250	0.1033	0.2391	0.2137	0.1716
C3	0.2234	0.0173	0.1125	0.0060	0.0430	0.0203	0.0437	0.1318	0.0265	0.0338	0.0658
C4	0.1257	0.0298	0.1172	0.1289	0.0658	0.0356	0.1996	0.1221	0.0663	0.0877	0.0979
C5	0.0050	0.0010	0.0031	0.0019	0.0023	0.0015	0.0047	0.0035	0.0002	0.0006	0.0024
C6	0.1891	0.0948	0.2128	0.0297	0.1812	0.1312	0.1468	0.0724	0.0749	0.1906	0.1324
C7	0.0019	0.0031	0.0066	0.0054	0.0013	0.0069	0.0011	0.0052	0.0045	0.0017	0.0038
C8	0.0673	0.1106	0.1110	0.1752	0.1248	0.0509	0.1204	0.0898	0.0938	0.0907	0.1034
C9	0.0362	0.0158	0.0392	0.0148	0.0445	0.0119	0.0337	0.0292	0.0290	0.0352	0.0290
C10	0.0012	0.0020	0.0010	0.0011	0.0007	0.0024	0.0006	0.0025	0.0023	0.0017	0.0016

Table 4.4: WINNER B3 scenario simulations when CDL model LOS case is used and $IntraClusterDsUsed$ is enabled.

In this table, the grey column represents the mean of all simulations and gives a general overview of the strongest and weakest cluster when the CDL model is used in case of WINNER B3 scenario. However, it makes clear the extent of cluster amplitude variability in each simulation, for example the third cluster in the first and fourth simulation. Like stated above, this problem is not controllable by the user, so requires special attention when comparing several simulations. This issue is addressed in the following sections.

4.2 Data analysis

This section aims to analyze the results obtained in [Vos08] with regard to IEM experiments conducted in the HCC hall. Subsequently, this analysis is compared with the WINNER channel model simulations carried out in the virtual scenario described in subsection 4.1.2. The WINNER simulations and the channel models comparisons are performed in the next sections.

As stated in chapter 1, in one of the IEM experiments conducted by [Vos08], a body pack, acting as a receiver (MS), is mounted on the belt of a test person who is located in the stage center, whereas that the transmitter antenna (BS) is placed in the upper left corner of the stage as can be seen in fig.3.12. Throughout these experiments, to measure the channel impulse response for different MS positions and in order to see the effect the test person body when it is located between both antennas, the test person, who is always in the center of the stage, turns on itself taking certain angles of rotation, 0^o(initial position), 45^o, 90^o, 135^o, 180^o, 225^o, 270^o and 315^o. [17] Fig 4.4 shows a diagram of the transmitter and receiver antenna locations used for the IEM experiments. The inset to the right to the stage describes all the different angles in which the test person is positioned.

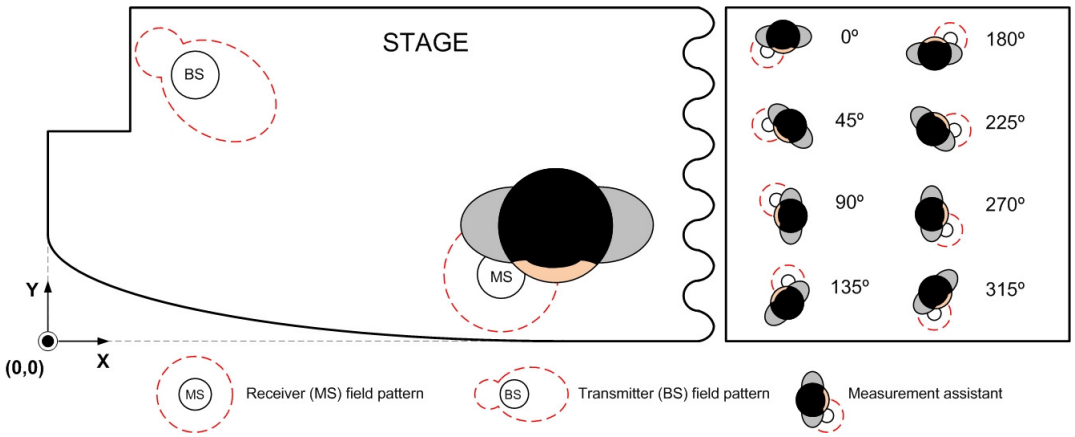

Figure 4.5: Scenario setup of the IEM measurements.

From all the data available presented in [Vos08], the analysis of this section is focused on the HCC hall CIR values obtained in the IEM experiments. This experiments were

[17] It is assumed that the center of the scenario is the center of the test person rotation.

conducted for a frequency band between 800MHz and 1800MHz, specifically for the following frequencies: 800MHz, 1000MHz, 1200MHz, 1400MHz, 1600MHz and 1800MHz. The channel impulse response data are stored in Matlab matrices. Each matrix contains 98 impulse responses for every center frequency and every position of the test person. Each impulse response is a vector composed by 1000 elements calculated with a frequency sampling interval of $delta_f = 200$kHz. The objective is to represent each Matlab matrix into a format so that, CIR data and the subsequent WINNER CIR simulations can be compared between them.

The main idea is to represent, in time domain, the impulse response for each MS position and for each center frequency. The method chosen is to calculate the average of the 98 impulse responses for every case, that is, transform each 1000x98 matrix into a vector of 1000 elements, where each element is the average of each matrix row. Each row can be expressed by $\bar{X}_i$, $1 \leq i \leq 1000$. To get a representative average, it is important to evaluate the variance of the data (each $\bar{X}_i$), because the higher the variance, the average is less relevant. The study of the variance is given by the standard deviation. The standard deviation of each $\bar{X}_i$ is obtained following the next expression.

$$\sigma_i = 10\log\sqrt{\frac{1}{N-1}\sum_{j=1}^{N}(x_{ij}-\bar{x})^2} \quad dB. \tag{4.5}$$

N is the number of CIR's for each MS position and for each center frequency, 98. x_{ij} is the jth element of $\bar{X}_i$ and $\bar{x}_i$ is the average of $\bar{X}_i$. The maximum standard deviation of $\bar{X}_i$, is calculated by this equation

$$\sigma_i\_max = 10\log(x_i\_max - x_i\_min) \quad dB, \tag{4.6}$$

where x_{i_max} is the maximum value of $\bar{X}_i$ and x_{i_min} is the minimum. As it is summarized in table 4.5, all standard deviations are acceptably low (less than $0.5dB$) to validate, in this case, the average method to represent each Matlab matrix.

From the impulse response representation, the most important task is to locate the clusters, but first it is necessary to determine the longest possible power delay profile. As reported

in [Fer87], high values of frequency resolution in measurements imply short periods of time for these measurements. This is directly related to the inversely proportional relationship between frequency and time,$t = 1/f$. As mentioned in the previous page, data from [Vos08] were taken with a frequency resolution of $\pm$200kHz which means that the longest PDP is $5\mu s$. Previously cited in [Sal], in indoor radio links, the multipath components (rays) arrive in clusters. Each cluster has its own decay time function independently of the overall impulse response decay function. Locating each group of rays, the approximate delay time of each cluster will be established.

Fig.4.5 presents the average of the impulse responses (in linear units) when the assistant is in the position of 90º at 800MHz.

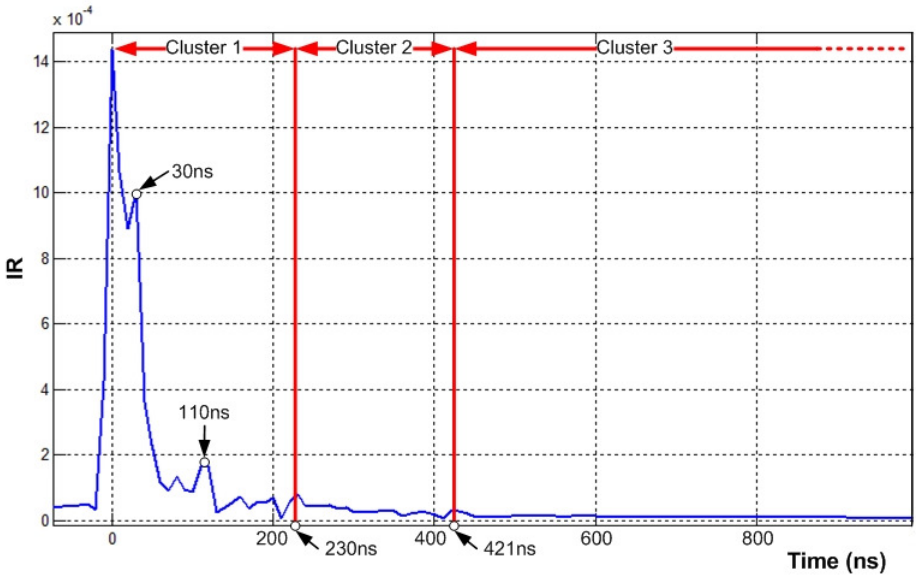

Figure 4.6: Impulse response at 800MHz when the MS is positioned at 90º.

This graph shows three clusters. The first is due to the direct ray between the transmitter and receiver. Inside the first cluster, there are two peaks at 30 ns and 110 ns. The first one is most likely caused by the signal reflection in the wall that is located one meter behind the BS(see fig.4.1). This assumption is based on the amplitude of this peak, which is near to the maximum IR level, and on the time delay, which is very close to the time delay of the direct ray. The second peak of the first cluster is probably due to the reflections in the columns of the left or right. Second cluster starts at 230 ns and is the result of the signal

reflection on the dividing wall, this means that the multipath component spends 230ns to reach the dividing wall and come back to the receiver traveling approximately 70 meters, 35 + 35 meters [18]. Third cluster begins at 421 ns and is due to the reflection on the back wall. In this case, the expected path length is 140 meters, 70 to reach the back wall and 70 to come back. As observed in fig.4.5, the relationship between the time it takes the first ray of clusters to reach the receiver and the distance traveled are the expected and logical one. In the same way, it concludes that the second peak of the first cluster, at 110 ns, is probably due to an approximate path of 34 meters which corresponds to the path from the transmitter to the receiver when the central columns located on the both sides of the part B of the hall(see fig.4.1) act as a reflectors agents.

The rest of the channel impulse responses at different center frequencies and MS positions, are analyzed and summarized in table 4.5 [19]. However, not all center frequencies are taken into account. As stated in chapter 3, the center frequencies of the antennas that are used to simulate the WINNER CIR are 900MHz and 1800MHz. For this reason and in order to obtain a realistic comparison between the two channel models, table 4.5 is focused only in the channel impulse responses measured at 800MHz, 1000MHz and 1600MHz. The features analyzed for the CIR's at 800MHz and 1000MHz are compared to the WINNER simulations when the antenna at 900MHz is used. Similarly, the CIR analysis at 1600MHz is contrasted with the WINNER CIR simulations at 1800MHz . The IEM experiments data at 1800MHz has been ruled out because for certain MS positions, 225^o, 270^o and 315^o, the signal level is to low and is therefore virtually impossible to detect the beginning of each cluster. Table 4.5 shows the time delay of each cluster [20]and the amplitude, A, of the first ray of each cluster [21]. Also includes $\bar{\sigma}$, which is the average of σ_i for each frequency and each MS position. The last CIR feature presented in this table is the maximum amplitude of each CIR, A_{max}, which corresponds to the first ray to reach the receiver.

[18] It is assumed that the first ray of the second and third cluster travels by a more or less straight path since it is the shortest path and hence the first to come back to the receiver.

[19] As mentioned above, each CIR is an average of the 98 CIR's which are stored in the Matlab matrices for each MS position and frequency.

[20] It is assumed that the first cluster always started at $t = 0$.

[21] The first ray of a cluster has the higest value of amplitude. For this reason, is easy to compare the amplitude of two clusters by comparing their first rays.

		2nd cluster		3rd cluster			
Rot(°)	f(MHz)	Delay(ns)	A(dB)	Delay(ns)	A(dB)	$\bar{\sigma}$ (dB) [22]	A_{max} (dB)
0	800	200	-40.92	370	-43.97	-60.7897	-30.85
45	800	220	-44.62	400	-45.53	-61.2280	-27.69
90	800	230	-40.99	420	-45.37	-59.1302	-28.53
135	800	230	-46.68	390	-47.09	-63.2499	-30.59
180	800	260	-49.57	430	-47.86	-62.3749	-30.93
225	800	240	-47.58	380	-48.77	-64.9868	-35.40
270	800	250	-44.45	360	-44.14	-62.8004	-35.52
315	800	240	-44.13	370	-42.87	-62.5672	-35.02
0	1000	230	-42.49	381	-43.14	-63.1891	-30.66
45	1000	200	-41.55	380	-43.83	-60.4853	-27.44
90	1000	190	-42.17	390	-44.09	-59.6505	-28.53
135	1000	200	-41.96	390	-44.89	-60.4126	-29.58
180	1000	200	-40.92	441	-47.26	-61.7742	-30.60
225	1000	190	-42.27	380	-44.35	-64.4793	-36.15
270	1000	210	-41.29	371	-42.31	-64.3783	-35.87
315	1000	210	-42	380	-41.90	-63.5511	-34.55
0	1600	220	-46.05	370	-48.06	-64.8526	-37.28
45	1600	220	-47.03	370	-51.26	-62.7157	-33.58
90	1600	220	-47.70	420	-55.08	-64.8142	-32.11
135	1600	200	-48.66	320	-51.68	-62.8341	-32.32
180	1600	220	-48.41	400	-52.74	-63.5552	-35.57
225	1600	180	-49.11	310	-52.71	-65.1234	-41.23
270	1600	220	-50.24	360	-50.65	-64.9775	-40.08
315	1600	230	-46.71	370	-49.65	-64.7145	-39.29

Table 4.5: Impulse response information from measurements in HCC hall

From table 4.5 it can draw some conclusions. When the mobile station is located in the angles 45°, 90° and 135°, the average of impulse responses for 800, 1000, and 1600 MHz reach the highest amplitudes. This can be seen in the last column of the table 4.5 that refers to the A_{max} which, in turn, matches with the beginning of the first cluster, that is, the direct ray between both antennas. In the same way, the lowest values of A_{max} correspond to angles 225°, 270° and 315°. This feature can be better understood looking at fig.4.5, in which the BS has a direct view of MS for the angles 45°, 90° and 135°, whereas that in the angles 225°, 270° and 315° there is an obstructed line of sight between transmitter and

receiver because of the test person body. The third cluster which is due to the reflection of the signal in the back wall, reaches its highest values, in all cases, for the angles 0º, 270º and 315º. These angles correspond to the MS positions that most directly point to the back wall. The amplitude of the second cluster first ray which correspond with the signal reflection in the dividing wall, do not follow a particular pattern. This may be due to reflections in the side walls, columns or both, before the arrival of the transmitted signal to the receiver MS.

Table 4.6, based on table 4.5, compares the amplitude of each cluster first ray, for the same frequency, by calculating the average of each cluster, $\bar{A}$, in all MS positions.

	1st cluster		2nd cluster		3rd cluster	
Frequency(MHz)	$\bar{A}$ (dB)	a_1	$\bar{A}$ (dB)	a_2	$\bar{A}$ (dB)	a_3
800	-31.81	1	-45.03	0.7	-45.7	0.69
1000	-31.67	1	-41.83	0.75	-43.97	0.72
1600	-36.43	1	-47.98	0.76	-51.47	0.70

Table 4.6: Clusters first ray amplitude comparison from measurements in HCC hall

a_1, a_2 and a_3 are the normalization factors of the first, second and third cluster respectively. a_1 is equal to 1 and, as mentioned above, represents the amplitude of the first cluster first ray. It can be seen that the higher the frequency, the greater is the second cluster in relation to the first cluster, while the relationship between the first and the third cluster is practically the same for all frequencies. On the other hand, the frequency of 1000MHz presents the higher values for both clusters and the 1600MHz exhibits the lower ones. Fig.4.7 shows graphically the amplitude relationship of each cluster first ray for all frequencies.

The cluster delay time features for 800, 1000 and 1600MHz are summarized in table 4.7. This table includes an overview of the cluster time delay information from table 4.5. Thus, for each frequency there is an interval in which both clusters appear regardless of the MS position. Also includes the mean of each interval and the standard deviation, σ.

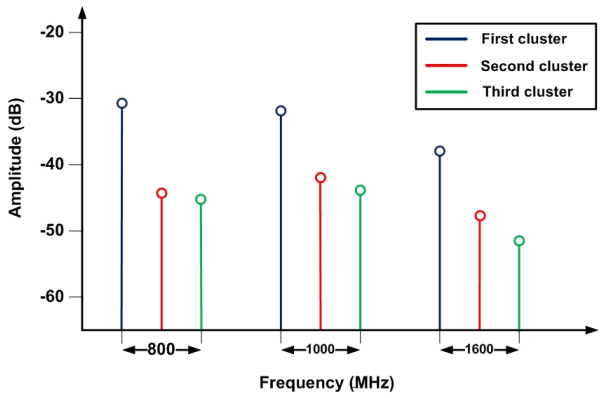

Figure 4.7: Clusters first ray amplitude comparison from measurements in HCC hall

	2nd cluster			3rd cluster		
Frequency(MHz)	Interval(ns)	Mean(ns)	σ(ns)	Interval(ns)	Mean(ns)	σ(ns)
800	200-250	$\approx$ 234	18.46	360-430	390	25.07
1000	190-230	$\approx$ 204	13.02	371-441	$\approx$ 389	21.83
1600	180-230	$\approx$ 214	15.97	310-420	365	36.64

Table 4.7: Clusters time delay features from measurements in HCC hall

For all the cases, the total range of time in which it is expected that the second cluster appears is between 180 and 250 ns. For the third cluster, the analysis concludes that the signal from the back wall takes 310 to 440 ns to reach the receiving antenna. For further information about the delays, the table 4.7, extracted from [Vos08][23], relates the time delay of several paths with the reflection points in which it is assumed that these paths are reflected towards the receiver.

This table only differs from the initial analysis in the fact that the time delay of the third cluster is extended a little bit more, up to 500 ns. For the comparisons with the WINNER channel model, both tables, 4.7 and 4.8, are taken in mind.

[23]This table is part of an analysis carried out in [Vos08].

	Columns				Dividing wall	Back wall
Time Delay (ns)	63	80	107	133	233	450 to 500
Distance (m)	9.5	12	16	20	35	70 to 75

Table 4.8: Path time delay as a function of distance traveled.

Fig.4.8 shows a simulation of the impulse responses for each frequency, 800, 1000 and 1600MHz, based on tables 4.5, 4.6[24], 4.7 and the Matlab data provided by [Vos08]. As explained in the beginning of chapter 4, these impulse responses belong to the IEM PWMS application experiments in which the transmitter antenna, BS, is located in the corner of the stage (see fig.4.1) and points to the stage center in where the receiver antenna, MS, is placed. The MS do not move from its position but can rotate 360^{o}.

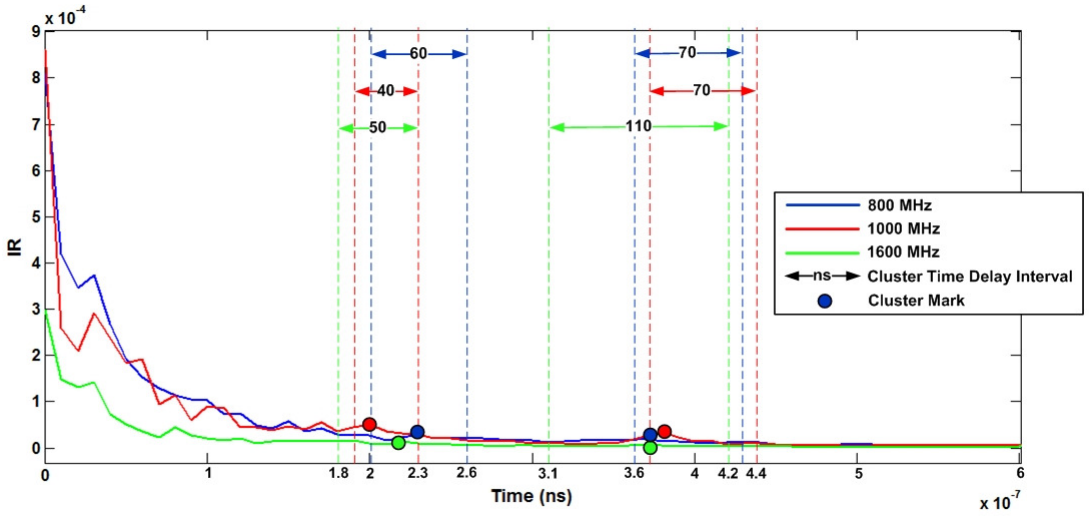

Figure 4.8: Impulse responses representation at 800MHz, 900MHz and 1600MHZ

Comparing the three impulse responses, it can be observed that the time delay of the second cluster increases with the frequency while the time delay of the third cluster decreases. The impulse responses corresponding to the frequencies of 800MHz and 1000MHz have the highest cluster amplitudes while the impulse response at 1600MHz exhibits the lowest ones. This may occur because the wavelength of the signal at 1600MHz is smaller

[24]The amplitude is expressed in linear coordinates to facilitate visualization.

(see equation 2.2) than the wavelength of the signals at 800 and 1000MHz. As mentioned in chapter 2, the shorter the wavelength of a signal, the more likely to be reflected and diffracted. This is because the electric size of the hall structure and elements is greater the shorter the wavelength of the signal incident. All this conclusions have to be confirmed or not, by comparing the data analyzed in this section with the simulations performed below using the WINNER channel model.

4.3 WINNER channel model simulations

In this section, the results of WINNER channel model simulations are presented and analyzed. This simulations are carried out in Matlab, using the WINNER Matlab code provided by [Narb] and explained in chapter 3. The goal is, also, to compare these simulations with the data obtained from [Vos08], and analyzed in subsection 4.2. This task is not easy because both data analyzed are based on statistical channel models whose parameters or typical values are the result of measurement campaigns carried out in similar indoor environments but not identical. In addition, the limitations of Matlab code largely restrict the description of the simulation layout.

In general, the WINNER Matlab code output is a channel impulse response matrix featured by a number of clusters [25], their amplitude and time delay and the time variance of the channel. This last characteristic depends on equation 3.16, and, as can be explained in subsection 3.2.3, high values of the parameter *SampleDensity* produce a CIR matrix stationary in time. Fig.4.9 shows two examples of channel impulse response matrices generated by the WINNER Matlab code. The example (a) is a CIR matrix variant in time, while example (b) is a stationary CIR matrix. The number of clusters is determined by the B3 LOS case WINNER scenario. This CIR matrix is not an appropriate format when it is compared with other simpler models, so in order to simplify the WINNER output, the mean of each cluster is calculated, obtaining the channel impulse response represented on the right of each CIR matrix in fig.4.9, in where each stem represents a cluster. This format is the same as showed in fig.4.4, but not the same as presented in fig.4.2 in which

[25] This parameter depends on the WINNER scenario chosen and its propagation condition, LOS or NLOS.

each stem is not a cluster, but a ray. The WINNER simulations conducted in this chapter are carried out in this way.

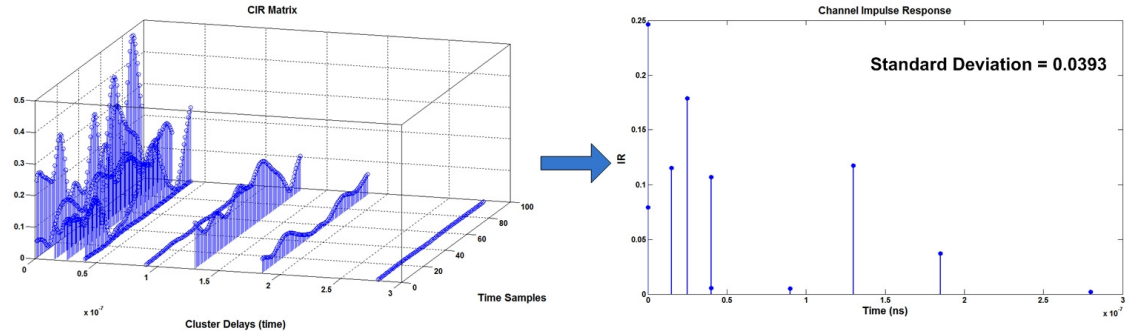

(a)

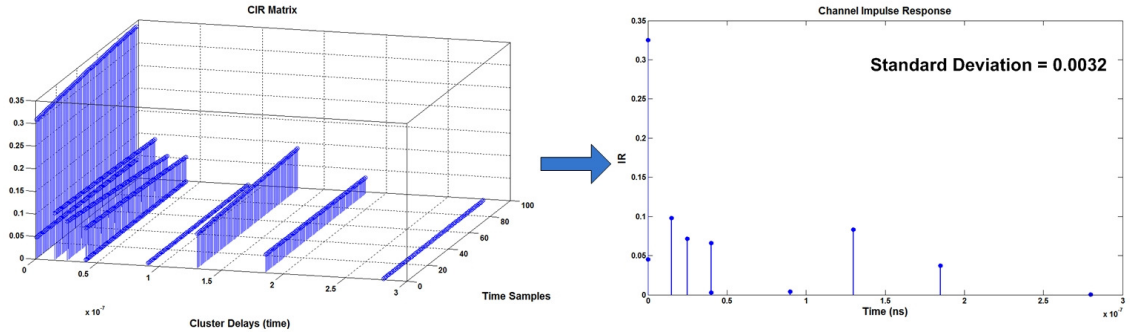

(b)

Figure 4.9: (a) Non stationary WINNER channel impulse response matrix; (b) Stationary WINNER channel impulse response matrix

The next subsection implements and analyzes the WINNER simulations based on the IEM experiments layout presented in section 4.2. Finally, the last subsection examines, for the same layout as above, the impact on the impulse response when the receiving antenna is on movement.

4.3.1 IEM WINNER analysis

Fig.4.11 describes the layout scheme used to implement the WINNER channel model realizations. The mobile station, MS, represent the test person with the body pack. To simulate the rotation of the test person, the MS is placed at different positions along a

radius of rotation of 30 cm. This radius simulates the width of the waist of the test person. Each MS position is equivalent to an angle of rotation, that is, while in the experiments conducted in [Vos08], measurements were taken to eight different test person angles of rotation [26], 0º, 45º, 90º, 135º,180º,225º,270º and 315º, in the WINNER simulations each angle corresponds with certain coordinates values in GCS as can be shown in fig.4.11. Another issue to consider is that, in real experiments, for the angles 180º, 225º, 270º and 315º, the test person body blocked the direct path between the transmitting and receiving antennas, creating an OLOS propagation situation. In order to simulate this case using the WINNER Matlab code, the propagation condition used to calculate the CIR, for the MS positions corresponding with those angles, is the NLOS[27] condition. In the same way, the MS positions corresponding with 0º, 45º, 90º and 135º, are evaluated under LOS propagation condition.

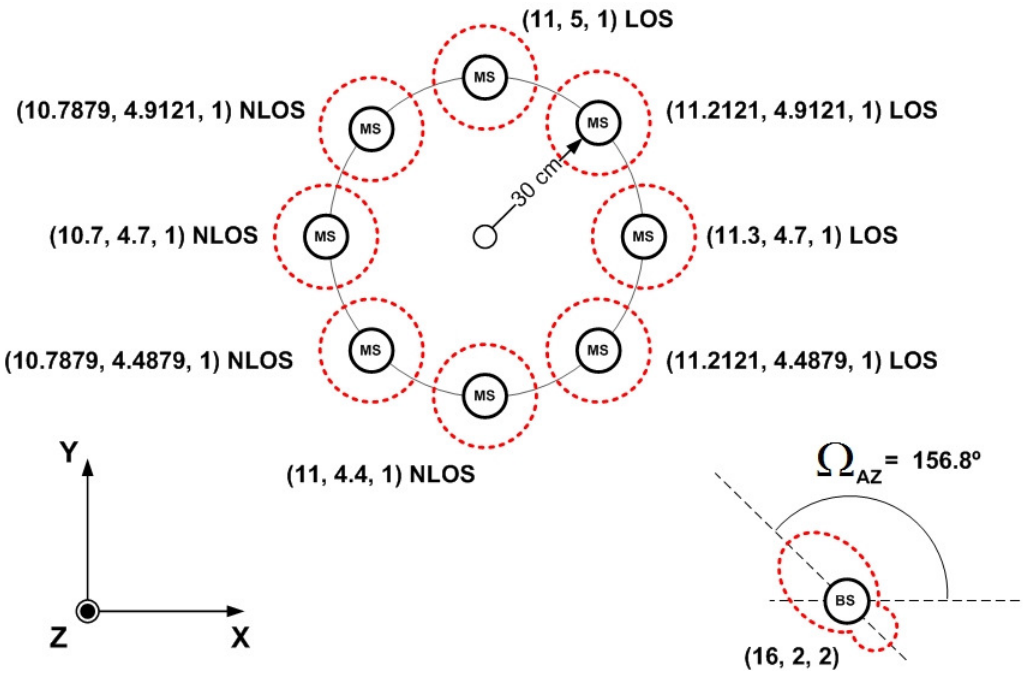

Figure 4.10: IEM WINNER layout configuration options

[26] See fig.4.5.

[27] NLOS is the nomenclature used by the WINNER channel model to describe the OLOS propagation condition.

The WINNER channel model is simulated for each MS position and for each type of transmitting antenna field pattern which is, as can be seen in subsection 3.2.1, implemented based on real models, one at 900MHz and the other one at 1800MHz. In all, for the IEM case, there are 16 different WINNER layouts configurations to simulate. For this purpose the WINNER B3 generic model is used. This means that one WINNER CIR simulation generates random cluster features based on probability density functions. The problem is that only one simulation do not give so much information about each specific layout case, and makes impossible to distinguish the impact on the CIR caused by different MS positions, antenna field patterns or propagation conditions. Therefore, it is necessary to generate enough amount of information for each layout configuration, that permits derive conclusions about each case, thus obtaining an overview of the whole IEM setup.

For each MS position and for each antenna field pattern, the main WINNER Matlab code file, *wim.m*, which is responsible of calculating the CIR, is executed 500 times[28]. This generates 500 random power delay profiles composed by 14 or 19 [29] clusters, depending on the propagation condition. The clusters are featured by their respective time delays and normalized amplitudes. All time delays obtained from each PDP, its occurrence and the mean of all normalized amplitudes associated with them, characterize the channel behavior for each layout configuration. Finally, and before execute the WINNER code, it is essential to define the velocity of the MS and BS station as well as the number of time samples and their time duration. In the IEM experiments conducted in [Vos08], the velocity of both stations was zero. In the WINNER Matlab code, while the velocity of the BS station does not have any restrictions, the MS velocity can not be set to zero as can be explained in subsection 3.2.2. For this reason, the Ms velocity is set to a value too low, so that it can be assume that the station is not moving. This value greatly increases the time sample interval as can be deduced from eq.3.16. However, the *SampleDensity* value for IEM WINNER simulations is set to 100. This value causes the CIR is practically stationary in time, thus making irrelevant the number of time samples and the time sample interval. By default the number of time samples is 98 [30].

[28] This number achieves a good compromise between the quality of information collected and the computational efficiency.

[29] In the WINNER IEM simulations, the WINNER control parameter $IntraClusterDsUsed$ is enabled.

[30] It is the same number as that used in the data analyzed in Section 4.2

In order to interpret a whole all WINNER Matlab code simulations for all layout configurations depicted in fig.4.11, fig.4.12 shows all cluster time delays appeared in the simulations and their typical normalized amplitudes. To complete the analysis, fig.4.13 represents the histogram in which the occurrence frequency of each cluster is presented.

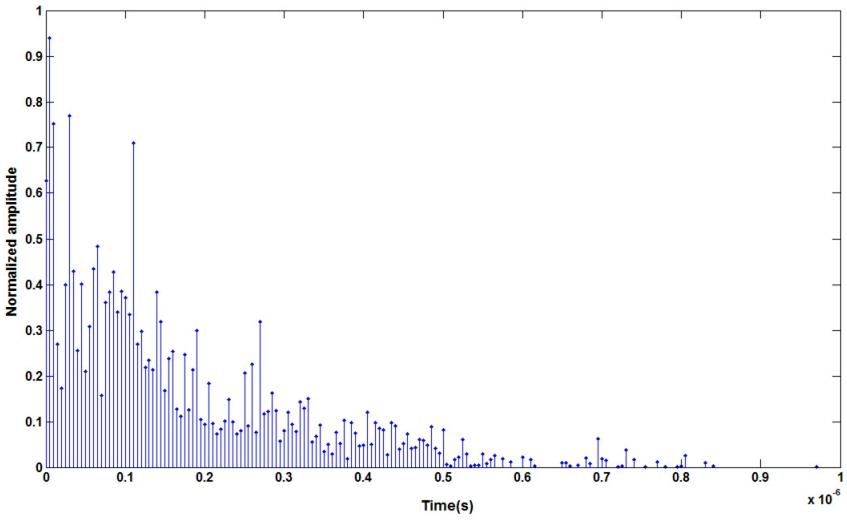

Figure 4.11: IEM WINNER clusters overview

The time interval in which are located all the clusters is between 0 ns and 900 ns. However, the clusters whose time delay is part of the interval from 400 ns to 900 ns, only represents the 0.562% of all the clusters obtained in the simulations. Moreover, the 97% of all clusters is between 0 and 250 ns. From this first analysis, it can be observe that in an indoor environment characterized by the layout configurations explained above, the WINNER channel model generally simulates a channel impulse response in which the strongest clusters are located in the first 100 ns. These clusters are the result of signal reflections or diffraction on scatter agents placed near to the receiving antenna. It can be observe, also, that the last significant clusters emerge in the time interval from 200 to 300 ns and correspond to 4.5% of the total of clusters. Because of its low level of occurrence and amplitude, the clusters obtained from 400 ns are not a significant feature of indoor channel WINNER simulations and therefore they are not so relevant. In summary, although there are clusters beyond 400 ns, it can be conclude that the channel impulse

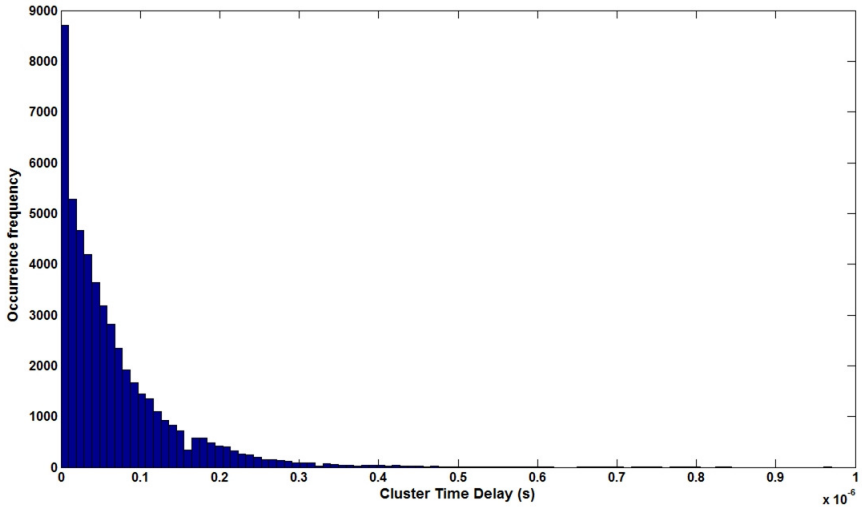

Figure 4.12: IEM WINNER clusters occurrence frequency

response for indoor environments simulated using the WINNER Matlab code, does not present significant multipath components beyond 400 ns, while, inside the interval from 0 to 150 ns, are placed the strongest paths. On the other hand, it must take into account that this analysis is an overview, since, the WINNER channel model is a statistical channel model and its CIR calculations are random simulations in each case.

The big difference between the [Vos08] channel impulse responses and the WINNER channel impulse response are located in the channel delay spread features. The analysis of both power delay profiles reveals that the delay spread from [Vos08] is at least double that the delay spread from WINNER model, since the amplitude and occurrence frequency of the WINNER multipath components beyond 250 ns, are practically negligible. However, with respect to the frequency and amplitude characteristics, any conclusion about the difference between both channel model realizations is too consistent and therefore not very useful. One of the reasons is the simulation limitations that WINNER Matlab code imposes. For example, there are no relevant differences between the 900MHz IEM WINNER simulations and 1800MHz IEM WINNER simulations. This is because of the center frequency relevance is found only in the field patterns of antennas, which, as seen in fig.3.10, are very similar, causing thus, unlike the data analyzed in section 4.2, that

from WINNER simulations, no conclusions can be drawn about how the different field patterns affect the channel impulse response. This issue and the layout design limitations of WINNER Matlab code significantly complicate the comparisons between the power delay profiles obtained in [Vos08] with the PDP's obtained using the WINNER channel model.

4.3.2 MS velocity analysis

The Saleh-Valenzuela channel model was developed under the assumption that the terminals, either transmitters or receivers, were fixed in one position, that is, they did not have velocity. This is a limitation when it tries to simulate an environment in which it is assumed that at least one station is on movement. In the experiments conducted in [Vos08], there were two stations inside the application scenario, both fixed in a certain position. This feature made that the stations velocity limitation of the Saleh-Valenzuela model was not a problem. The thesis at hand, has used the WINNER channel model to simulate a scenario as like as possible that the simulated in [Vos08]. The difference is that the WINNER model has been designed, unlike the Saleh-Valenzuela model, to simulate environments in which the stations may be moving. This characteristic has motive the analysis of how the Ms velocity can affect the channel impulse response of the PWMS scenario described in subsection 4.1.2.

In the IEM PWMS application described along this report, the only movement possible would be the test person walking on the stage with the body-pack in his belt. This means that, while the BS is fixed, the MS could move with a velocity between 0 and 5 Km/h. Moreover, in the measurements campaigns carried out to define the WINNER B3 scenario parameters the velocity of the stations did not exceed 5 km/h. These features make that the MS velocity range to be analyzed in this section is between $(0,5]km/h$. However, to see the effect of the MS velocity in the power delay profile of the channel, it is necessary to take into account the limitations of the WINNER channel model.

As presented in last sections, the WINNER model is a deterministic channel model that randomly generates cluster features based on probability density functions. For testing purposes, such as those discussed in this section, it is essential to reduce the randomness

of the simulations as much as possible. For this reason, the B3 generic model is not the appropriate model because, for the same layout setup, the simulations vary substantially from each other, causing thus, that the potential effects, in the CIR, of the MS velocity modifications are concealed. As explained in chapters 3 and 4, the WINNER CDL models fix the values of the delays, power and angle cluster features according to CDL tables. In this way, this is the suitable WINNER simulation option for testing purposes since considerably reduces the randomness of each simulation. The problem is that not all cluster parameters are given by the CDL tables. The Ricean k factor, shadow fading and rays (within each cluster) angle features are still random parameters, and as it can be concluded from table 4.4, produce amplitude fluctuations in each simulation under the same conditions. WINNER simulations with different MS velocity from 0 to 5 km/h not result in significant amplitude variations that can be separated from the amplitude changes produced by the randomness of those parameters. Therefore, for the same WINNER layout configuration and using the CDL tables, different MS velocities from 0 to 5 km/h can not drawn specific conclusions about changes in the clusters amplitude and delay time [31]. Nevertheless, there is still a field for analysis, the time evolution of the channel impulse response.

The time evolution of the CIR, depends on the number of time samples and the time duration of each one. Since the number of time samples is a fixed value, the WINNER simulation parameter that determines the channel time evolution is $delta\_t$. In turn, as can be seen in subsection 3.2.3, $delta\_t$ depends on the center frequency, $SampleDensity$ and MS velocity. $SampleDensity$ and frequency are also fixed values so, in summary, the MS velocity determines the time duration of each time sample and therefore the time variation of the channel impulse response. The next table summarizes the time sample duration for each value of MS velocity [32]. The simulations are carried out for the IEM layout at 900MHz when the test person is located with the angle of 0^o. The number of time samples are 98 and $SampleDensity = 2$.

In real measurements, the time sample interval usually is a fixed value as, for example, in [Vos08] experiments. WINNER varies this parameter as a function on the MS velocity. Consequently, the time evolution of the channel impulse response does not change con-

[31] The clusters delay time values are set by the CDL models.
[32] From 0 to 5 Km/h. in steps of 1 Km/h

MS Velocity (km/h)	delta_t (s)
$1e{-}5$	$3e4$
1	0.3
2	0.15
3	0.1
4	0.075
5	0.06

Table 4.9: Relationship between MS velocity and $delta\_t$.

siderably with different MS velocities. To simulate real measurements, the Matlab code responsible for calculating $delta\_t$ is replaced by another in which $delta\_t$ is not a function of MS velocity but a fixed value of 0.1 seconds [33]. This change takes place within the WINNER Matlab file *wim_core.m*.

$$delta\_t = \frac{\lambda}{2(v_{MS} \times sd)} \Longrightarrow replaced\ \ by \Longrightarrow delta\_t = 0.1 \tag{4.7}$$

To observe, graphically, the time evolution of the CIR, that is, the time evolution of each cluster, the three clusters [34] with the higher values of amplitude are selected to be plotted in Fig.4.13. This figure is similar to fig.3.15, but in this case the cluster time evolution is calculated as a function of the MS Velocity, and not as a function of the parameter *SampleDensity*.

Fig.4.13 shows that the higher the MS velocity, the greater the amplitude fluctuations of the clusters. That is, the channel impulse response is more variable over time. As cited in [Rap02], the coherence time T_c is the parameter used to characterize the time varying nature of the channel in the time domain. The definition of this parameter is shown in the next equation:

$$T_c = \frac{0.423}{f_m}, \tag{4.8}$$

[33] This is the central value of $delta\_t$ from table 4.9, and allows to see the variability of the CIR time evolution for MS velocities bigger and smaller than 3 m/s.

[34] The rest of the clusters do not be selected because they do not provide extra information and may blur fig.4.13.

in where f_m is the maximum Doppler shift given by

$$f_m = \frac{v_{MS}}{\lambda}. \tag{4.9}$$

In a wireless transmission, if the symbol rate of the transmitted signal is lower than $1/T_c$, the channel will cause distortion in the receiver. Thus, for a fixed center frequency, equations 4.8 and 4.9 determine that the greater the MS velocity, a greater symbol rate is necessary to avoid distortion in a wireless application, such as, the PWMS application under consideration in this thesis. For example, for a frequency of 900MHz, the relationship between the symbol rate and the MS velocity must be:

$$S_{rate} > \frac{0.423\lambda}{v_{MS}} \quad \textit{to avoid distortion}. \tag{4.10}$$

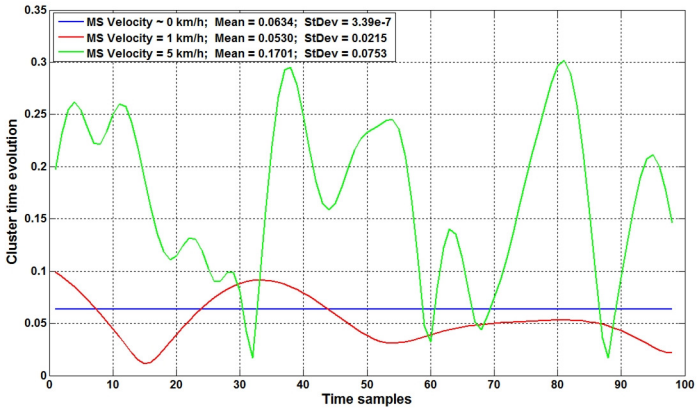

(a)

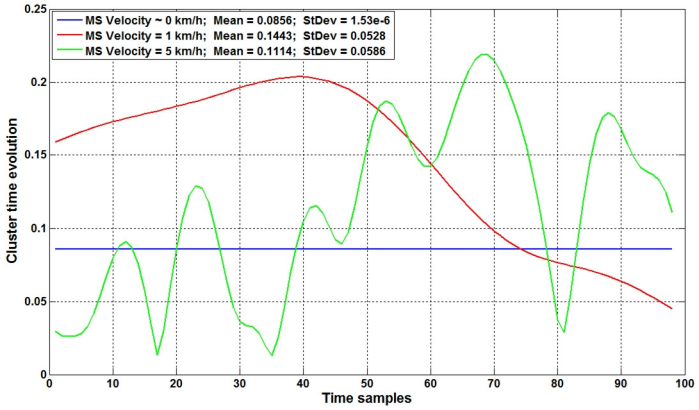

(b)

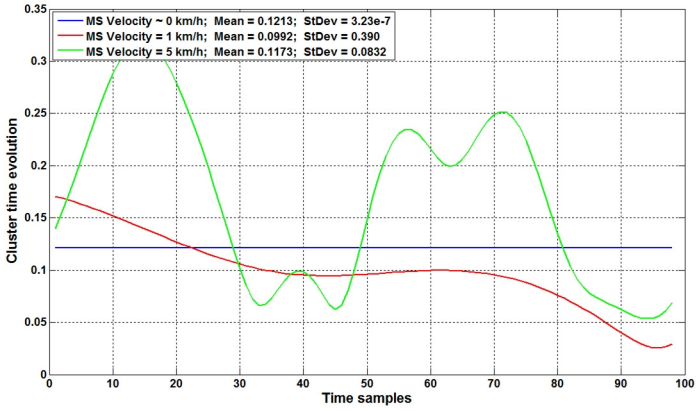

(c)

Figure 4.13: Relationship between cluster time evolution and MSVelocity.

5 Summary, conclusions and outlook

This thesis has been developed in order to extend a previous research [Vos08], in which a specific professional wireless microphone system (PWMS) application had been studied and analyzed. As a reminder, this PWMS application is based on the in ear monitoring IEM system which is composed by a fixed transmitting antenna and a body pack acting as a receiver. In [Vos08], real measurements of that application were taken inside the Hannover Congress Center hall. Data obtained were analyzed and modeled using the Saleh-Valenzuela channel model. This thesis extends that report, by using the WINNER channel model to simulate the same PWMS application.

The first thing conducted, has been a study of the theoretical degrading effects that occur inside an indoor wireless communications system and the basic features description of the main channel models involved in this thesis, the Saleh-Valenzuela model and the WINNER channel model. These descriptions have been presented in chapter 2. Since the WINNER simulations are carried out in MATLAB, [ist] provides the MATLAB code necessary to implement the channel impulse response realizations. Chapter 3 is responsible for delving into the WINNER Matlab code and shows all the configuration possibilities offered. In the last part of this chapter, it is summarized the configuration options that are relevant to simulate the PWMS application. Moreover, it is also proposed the appropriate values of each WINNER code parameter, in order to adjust the WINNER simulation environment as close as possible to the HCC hall. The key chapter of this thesis is the chapter 4. From all the WINNER configuration options, chapter 4 describes the application scenario in which WINNER simulations are implemented. Also, based on the description of the HCC hall structure and based on the data provided by [Vos08], chapter 4 analyzes the power delay profile features concluded in that report. Finally, the WINNER channel im-

pulse response simulations are performed taking into account the WINNER Matlab code configuration options established.

Since the WINNER channel model is a statistical model, to obtain conclusive results, many simulations have been carried out for each WINNER layout configuration and for each frequency, specifically, 8000 WINNER executions. This issue leads to the use of statistical tools, such as the mean and the standard deviation, to analyze the whole setup. The mean has been used to transform the WINNER channel impulse matrix into a simple and more representative power delay profile or channel impulse response, excluding to analyze the time evolution of channel that, in general, is not relevant in this thesis. The mean is also use to do an average of the amplitude of all clusters with the same time delay, thus giving an idea of the cluster amplitude level as a function of cluster time delay. From all WINNER executions, the frequency of occurrence of each cluster has been studied and depicted by a histogram.

Oblivious to the data analyzed in section 4.2, the effects of the receiver MS velocity in the PDP has been investigated. This work has been motivated by the fact that the WINNER cannel model has been developed to support mobility of the stations involved in the wireless communication links. In this section, 100 WINNER executions are carried out for three different MS velocities. However, due to the WINNER Matlab code limitations, it has been necessary to make changes in the original WINNER Matlab code in order to unify the time sample duration of each simulation, and thus, visualize the changes in the channel time evolution. The main conclusion is that, for a fixed simulation time, the higher the MS velocity, the greater the fluctuation of the channel. In other words, when the MS velocity is increased, higher symbol rates are required to avoid distortion in the receiver

In the IEM case, when comparing the data analyzed from [Vos08] with the power delay profiles obtained in WINNER simulations, the first noteworthy difference is that, for a similar application scenario described as a conference hall or concert room, the WINNER channel model locates the main components of the multipath propagation (clusters), inside an interval from 0 to 250 ns, while the Saleh-Valenzuela extends these multipath components (rays)up to 500 ns. That is, the total delay spread of Saleh-Valenzuela model is approximately twice that the delay spread obtained from WINNER realizations. How-

ever, for amplitude characteristics both models can be analyzed separately but not together because of the amplitude units differences between them. At best, it can be concluded that both models exhibit the highest amplitude values in the first multipath components. Furthermore, unlike Saleh-Valenzuela model, WINNER model assumes strong multipath components in the middle of its total delay spread. Actually this analysis is only an overview. The main reason is that the results of WINNER simulations are conditioned to limitations of WINNER Matlab code and to the statistical nature of the WINNER channel model. The randomness of the WINNER parameters makes the analysis of the WINNER impulse response obtained, not accurate enough to compare in detail with other models, such as in this case.

Although the CDL model tables are used, there are always a few random parameters, and, since the different WINNER layouts are based on small changes in the position and field pattern of each antenna, this little randomness is enough to mask the effects of those layout changes. To improve this thesis may be a solution, to investigate very thoroughly the key WINNER Matlab files and modify the WINNER code in order to achieve the full control of the simulation randomness.

Although the CDL model tables are used, there are always a few random parameters, and since the different WINNER layouts are based on small changes in the position and field pattern of each antenna, this little randomness is enough to mask the effects of those layout changes. To improve this thesis may be a solution, to investigate very thoroughly the key WINNER Matlab files and modify the appropriate WINNER code in order to achieve the full control of the simulation randomness.

Another possible way of improving is to use deterministic channel models such as ray tracing. This model solves the problem that WINNER channel model presents when it tries to emulate specific simulation scenarios. The ray tracing, based on geometrical optics, allows the user to describe in detail each kind of scenario, making more real the comparisons between different channel models.

To end this thesis, as stated in section 2.5.2, COST 273 may be a suitable statistical channel model to simulate the PWMS application presented in previous chapters. This model seems to be the same problems as WINNER model but can extend the information about the indoor channels simulations, and perhaps can provide new findings.

Bibliography

[Alm] ALMERS, P.; ET AL.: «Survey of Channel and Radio Propagation Models for Wireless MIMO Systems ». In: *EURASIP*

[Cav00] CAVERS, J.K.: *«Mobile Channel Characteristics»*. Kluwer Academic Publishers, 2000

[Fer87] FERNÁNDEZ, J.: *«Instrumentos de medida eléctrica»*. Editorial Reverté S.A., 1987. – ISBN 84–291–6054–X

[Has] HASHEMI, H.: «The Indoor Radio Propagation Channel ». In: *IEEE*

[HCC] *Hannover Congress Centrum*. `http://www.hcc.de`

[ist] *WINNER Phase II Model*. `http://www.ist-winner.org/phase-2-model.html`

[Kyöa] KYÖSTI, P.; MEINILÄ, J.; HENTILÄ, L.; ZHAO, X.; JÄMSÄ, T.; SCHNEIDER, C.; BAUM, D.; MILOJEVIC, M.; EL-SALLABI, H.; LASELVA, D.; NUUTINEN, J.; VAINNIKAINEN, P.; KIVINEN, J.; VUOKKO, L.; RAUTIAINEN, T.; ZETTERBERG, P.; BENGTSSON, M.; YU, K.; JALDEN, N.; KALLIOLA, K.; HANSEN, J.: «IST-2003-507581 WINNER D5.4 v.1.4 Final Report on Link Level and System Level Channel Models »/ Information Society Technologies. – Forschungsbericht

[Kyöb] KYÖSTI, P.; MEINILÄ, J.; HENTILÄ, L.; ZHAO, X.; TÄMSÄ, T.; SCHNEIDER, C.; NARANDZIC, M.; MILOJEVIC, M.; HONG, A.; YLITALO, J.; HOLAPPA, V.; ALATOSSAVA, M.; BULTITUDE, R.; DE JONG, Y.; RAUTIAINEN, T.: «IST-4-027756 WINNER II. D1.1.2 V1.1. WINNER II Channel Models »/ Information Society Technologies. – Forschungsbericht

[Lan] LANDMANN, M.; DEL GALDO, G.: «Efficient Antenna Description for MIMO Chanel Modelling and Estimation ». In: *IEEE*

[Mol] MOLISCH, A.; ZHANG, J.; KUZE, T.; FU, I.; FANG, L.; CHEN, S.; QU, H.: «Motivation for IEEE 802.16m channel model submission to ITU »/ IEEE 802.16m Group. – Forschungsbericht

[Nara] NARANDZIC, M.; KASKE, M.; SCHNEIDER, C.; MILOJEVIC, M; LANDMANN, M.; SOMMERKORN, G.; REINER, T.: «3D-Antenna Array Model for IST-WINNER Channel Simulations ». In: *IEEE*

[Narb] NARANDZIC, M.; KYÖSTI, P.; HENTILÄ, L.; KÄSKE, M: «Matlab SW documentation of WIM2 model »/ Information Society Technologies. – Forschungsbericht

[Par] PARVIAINEN, R.; YLITALO, J.; EKMAN, R.; TALMOLA, P.; HUUHKA, E.;: «Measurement Based Investigations of Cross-Polarization Characteristics Originating rom Radio Channel in 500MHz Frequency ». In: *IEEE*

[Rap02] RAPPAPORT, T.s.: *«Wireless Communications. Principles and practice »*. Prentice Hall, 2002

[Sak] SAKAR, TK.;JI, ZHONG.;KIM, KYUNGJUNG.;MEDOURI,ABDELLATIF.;SALAZAR PALMA, MAGDALENA.: «A Survey of Various Propagation Models for Mobile Communications ». In: *IEEE Antennas and propagation Magazine*

[Sal] SALEH, A.; VALENZUELA, R.: «A statistical Model for Indoor Multipath Propagation ». In: *IEEE*

[sch] *Schwarzbeck Mess - Elektronik*. `http://www.schwarzbeck.de/artikel.php?lang=1kat=AM`

[Skla] SKLAR, B.: «Rayleigh Fading Channels in Mobile Digital Communications Systems Part I: Characterization ». In: *IEEE Communications Magazine*

[Sklb] SKLAR, B.: «Rayleigh Fading Channels in Mobile Digital Communications Systems Part II: Mitigation ». In: *IEEE Communications Magazine*

[Skl01] SKLAR, B.: *«Digital communications: Fundamentals and Applications »*. 2nd edition, Prentice-Hall, 2001. – ISBN 0–13–084788–7

[Tur] TURIN, G.; CLAPP, F.; JOHNSTON, T.; FINE, S; LAVRY, D.: «A Statistical Model of Urban Multipath Propagation ». In: *IEEE Transactions on Vehicular Technology*

[Vos08] VOSS, D.; DORTMUND, S.: *«Modellierung schmalbandiger ÜbertragungsKanäle für drahtlose Audioübertragungssystema im Bühnenumfeld »*, Universität Hannover, Institut für Hochfrequenztechnik und Funksysteme, Hannover, Diplomarbeit, 2008

[Zha] ZHANG, Y.; ZHANG, J.; SMITH, P.; SHAFI, M.; ZHANG, P.: «Reduced Complexity channel Models for IMT-Advanced Evaluation ». In: *Journal on Wireless Communications and Networking*